# Responses to Comment of Referee #1

In its present form, the paper mostly appears as a good piece of algebraic development, and along this line, corresponds typically to a technical note. However, a few concerns make me feel that the writing is not raised to something braking from previous attempts to model unconfined groundwater flow.

First. Contrary to the idea concealed in the paper, I am not convinced at all that analytical solutions are in general the reference tool for concrete case applications. Usually, analytical solutions drastically simplify the problem when concrete applications are faced with complex situations. Todays, concrete application turn toward (eventually simplified) numerical resolutions of groundwater flow simply because these approaches can handle complex geometry, medium heterogeneity, coupling vadose and saturated zone, etc. The point is that analytical solutions are still useful as reference for numerical model and/or to assess the relevance of some second-order mechanisms added to numerical models.

Response: We agree that analytical solutions are reference tools for applications with complicated situations or serve as the primary means for testing and benchmarking numerical models or assessing the relevance of some second-order mechanisms included in numerical models. In addition, they have advantages mentioned below as compared with the numerical methods:

1. They generally require less data than numerical schemes and are numerically stable, efficient, and easy to implement although they are limited to specific cases due to their simplifying assumptions.
2. They can easily be used to explore physical insights of the flow behavior affected by the aquifer properties, boundary, and/or surface recharge. Some new findings related to flow behavior are given below as example based on the present solution:

(1) A quantitative criterion is provided to assess the validity of neglecting the effect of the vertical flow. Such a practice of ignoring vertical flow was very commonly made in previous articles (e.g., Rao and Sarma, 1980; Rai et al., 1998; Chang and Yeh, 2007; Illas et al., 2008). Please refer to the 2$^{nd}$ conclusion in the previous manuscript for detail.

(2) The assumption of incompressibility is valid when the ratio of the specific yield to the storage coefficient is larger than 100. Otherwise, it leads to significant overestimation in predicting the hydraulic head. Please see the 3$^{rd}$ conclusion in the previous manuscript.

3. The sensitivity analysis based on the analytical solutions can determine which parameters are relatively critical to the success of a management plan (see, for example, Aguado and Sitar, 1977) or to investigate the source of inaccuracy in parameter estimation (e.g., Huang and Yeh, 2012).

4. If coupling with an optimization approach, they can identify the hydraulic parameters in aquifer test data analyses. For example, Yeh and Chen (2007) integrated a slug test solution for a well with a finite-thickness skin with the simulated annealing to determine the hydraulic parameters of the skin and formation zones.

Second. I doubt on the unconfined behavior of the aquifer modeled by the solutions of the authors. For the purpose of simplification, the analytical solution is based on two equations, namely, a diffusion equation corresponding to a confined system plus an additional equation for the free water surface only accounting for fluxes from the recharge over a limited area of the modeled domain. It is obvious that this dichotomy does not represent the continuity of flow between the vadose and the saturated zone that makes the unconfined systems so complicated. The authors would have been well advised to provide us with a comparison between their solution (and its simplifications) and a full three-dimensional resolution of the Richards equation for both the saturated and the vadose zone. The point is not to state that an analytical solution is able to deal with all the physics of flow, rather to show explicitly why the simplifications needed for building an analytical solution are reasonably acceptable.

Response: Thanks for the comment. Analysis of three-dimensional saturated and unsaturated flows based on Richards' equation and soil characteristic curve is indeed an interesting and challenging work, but this is obviously beyond the scope of this note. Tartakovsky and Neuman (2007) developed a semi-analytical solution for unsaturated and saturated flows toward a discharge well in an unconfined aquifer. Their solution is based on Richards' equation with the relative hydraulic conductivity defined as $k_0 = \exp(-\kappa z)$ where $\kappa$ is a parameter and $z$ is elevation from water table. The solution agrees well with the Neuman (1974) solution based on the same problem but neglecting the effect of unsaturated flow when $\kappa B = 10^3$ with the initial aquifer thickness $B$. To some extent, the present work is similar to the Neuman (1974) solution but differs from the aspect that our solution regards regional recharge as a plane source while Neuman's solution considers the pumping as a line sink. We may therefore infer from the work of Tartakovsky and Neuman (2007) that the present solution may also be valid if the condition of $\kappa B \geq 10^3$ is held. The following text is added in the revised manuscript to address the conditions of using the present solution:

"On the other hand, the effect of unsaturated flow above water table on model's predictions can be ignored when $\sigma B \geq 10^3$ where $\sigma$ is a parameter to define the relative hydraulic conductivity as $k_0 = \exp(-\sigma z)$ in the Richards' equation (Tartakovsky and Neuman, 2007). Tartakovsky and Neuman (2007) achieved agreement on aquifer drawdown evaluated by their analytical solution based on Eq. (1) for saturated flow and Richards' equation for unsaturated flow and by the Neuman (1974) solution based on Eqs. (1) and (8) with $I = 0$ when $\sigma B = 10^3$ (i.e., the case of $\kappa_D = 10^3$ in Fig. 2 in Tartakovsky and Neuman, 2007)." (lines 176 − 183 of the revised manuscript)

Third. In association with the concern above, the provided analytical solution is compared with other analytical solutions grounded in the same theoretical framework. This way of doing usually goes with some self-satisfaction attitude because progresses are incremental and never work against the proposed methodology. Again, we would have been better informed if the proposed analytical solution had been faced with a (numerical) three-dimensional resolution of flow. It is now well known that solving a three-dimensional Richards equation with the problem of swapping between the unconfined non-saturated zone and the confined saturated zone is crux to model unconfined aquifers, especially when recharge is evoked as a condition triggering transient flow. Stated differently, one can be still interested in analytical solutions but it is mandatory to know when to apply them, what do they hide, and which (eventually useless) mechanism is overlooked. As an aside comment, we still seek for the usefulness of mixed boundary conditions when the paper only deals with the Dirichlet type of boundary condition.

Response: Unfortunately, it seems that the existing numerical solutions for 3D saturated and unsaturated flow were developed for some purposes (e.g., Dogan and Motz, 2005; Cey et al., 2006; Hunt et al., 2008; An et al., 2010; An et al., 2012) which were irrelevant to this study and therefore impossible to make comparison with the present solution. As regard to the use of the Robin boundary condition (RBC), we would like to mention that it is defined as a weighted combination of Dirichlet boundary condition and Neumann boundary condition while the mixed boundary condition (MBC) represents the boundary which changes its condition along a particular boundary, say from a Dirichlet condition to a Neumann condition (Duffy, 2008, p. 1). Thus, the RBC and MBC are completely different types. In our study, we have adopted the RBC to describe flow across a boundary of a stratum having low permeability and investigate its effect on the hydraulic head at an observation point as described in section 3.1. It is clear that the Robin condition should be considered for the boundary under the condition $10^{-2} < K_1 d_1/(K_x b_1) < 10^2$ where $K_1$ and $b_1$ are the hydraulic conductivity and width of the medium at the boundary 1 illustrated in Figure 1(a), respectively, $K_x$ is the aquifer hydraulic conductivity in the $x$ direction normal to the boundary, and $d_1$ is a distance between the boundary and the edge of a recharge area. Note that the Robin condition reduces to Dirichlet condition when $K_1 d_1/(K_x b_1) \geq 10^2$ and the no-flow condition when $K_1 d_1/(K_x b_1) \leq 10^{-2}$.

Four. Technically speaking, the manuscript may appear unclear at some places. The first question raised by reading the mathematical development is the motivation to choose a distance from a well as the reference for building dimensionless coordinates in space. What if no well existed? Why not to build theses dimensionless variables by taking the size (along x and/or y directions) of the domain? Is there any incompatibility by doing so on the emergence of an analytical solution? A second concern is about the sensitivity of the solution to parameters. The authors delineate it as a first order-approximation (finite difference) of the derivatives of the solution with respect to (log) parameters. This calculation is de facto sensitive to the increment $\delta$p added to the parameter p when approximating dF/dp as [F(p+$\delta$p) – F(p)]/$\delta$p. My understanding is that the analytical solution is a double or a triple sum of elementary functions. Derivatives of a sum being sum of derivatives, why not to derive directly the analytical solution with respect to parameters? My first guess is that all the elementary functions enclosed in the solution are differentiable with respect to their parameters, with the consequence that an "exact" sensitivity evaluation could come out by directly differentiating the analytical solution. Notably, the sensitivity analysis performed in the paper is irrelevant. Calculating derivatives with respect to parameters is always local, with the meaning that the differentiation is performed in the vicinity of a prescribed value of the parameter. Conclusions on model sensitivity are thus local and only valid close to the prescribed values of the parameters. These values are not reported in the paper and a relevant way to analyze the sensitivity would be to duplicate calculations at several points in the parameter space. A third concern is about the appendix which is in my opinion hard to read when it should be limpid. The reader is continuously invited to swap between the writing in the appendix and the equations in the main text. This does not help to understand how the authors technically proceeded for building their analytical solution. My standpoint regarding this feature would be to either remove the appendix, or give it some flesh to document the reader and avoid him back and forth motions in the reading plus hard time to pass from eq. n to eq. n+1.

Response: Thanks for the comment. Our responses to those concerns are given below:

1. The term "observation well" is changed to "observation point" for avoiding confusion. The distance $d$ between the edge of a recharge area and the observation point is chosen to define the dimensionless parameter $\kappa_z = K_z\, d^2/(K_x\, B^2)$ where $B$ is the initial aquifer thickness and $K_x$ and $K_z$ are the aquifer hydraulic conductivities in the $x$ and $z$ directions, respectively. The parameter $\kappa_z$ indicates that both $K_z/K_x$ and $d^2/B^2$ are crucial factors in neglecting the effect of vertical flow on the hydraulic head. This parameter is similar to the one defined in Neuman (1975) as $\beta = K_z\, r^2/(K_r\, H^2)$ with $K_r$

representing the hydraulic conductivity in the radial direction and $r$ denoting a radial distance measured from a pumping well to an observation point. He used this parameter to examine the validity of neglecting the effect of vertical flow on transient drawdown at the observation point (see Figure 1 in Neuman, 1975).

2. Direct differentiation of the solution with respect to each of the parameters is practically feasible. Yet, some of the results for parameters such as $S_y$, $S_s$, $K_x$, $K_z$, and $K_1$ are lengthy and in complicated forms. In addition, it is laborious to derive the sensitivity coefficients since we have seven parameters in total. The sensitivity coefficients based on the first-order finite differences give very good approximations to those obtained by direct differentiation. In addition, the curves of sensitivity coefficients show very clearly pictures exhibiting the relative strength and influential period of the impact of parameter change on the hydraulic head. The parameter values we choose and listed in Table 2 (in manuscript) are reasonable for sandy aquifers, which are suitable formations for groundwater exploitation. One might expect that different sets of parameter values for sandy aquifers should also provide similar sensitivity patterns to ours. The conclusions on the sensitivity analysis in section 3.5 should therefore be valid for different magnitudes of hydraulic parameters. It is worth noting that the patterns of sensitivity curves are somewhat different as shown in Figure 6 because Figure 6(a) is for three-dimensional flow while Figure 6(b) is for two-dimensional flow.
3. The derivation for the present solution mentioned in section 2.2 and given in Appendix A has been rewritten according to the comment and also given at the end of this reply.

Five. Even though I am not native speaker of English, I found a text riddled every ten lines with grammatical inconsistencies, awkward phrasings, etc. In any case, the manuscript would deserve pinpoint editing by a professional service. In its present form, the text is not completely clear and editing would probably improve readability.

Response: The manuscript has carefully been edited by a colleague who is good at English writing.

Finally, I found the paper interesting because the technique concealed in it is undoubtedly sound. The main concern is that the authors missed the target of showing us the added-value of their contribution. They partly kick in touch by comparing their results with those they inherit from. At least, the paper deserves a rigorous editing before publication. Nevertheless, my feeling is still that a relevant paper in a reputed journal such as HESS should argue on the advantages and drawbacks brought by the study. In its present form, the study only brings advantages by flawed comparisons between quite similar approaches. I would recommend to reject the paper in its present form but encourage the authors for a complete re-submission following the philosophy depicted above.

Response: Thank for the comment. We have addressed the issue of the restrictions (or drawbacks) of the present solution by inserting the following sentence in Conclusions of the revised manuscript:

"The present solution is applicable under the conditions of aquifer homogeneity, $|h|/B < 0.5$, $I/K_z < 0.2$, and $\sigma B \geq 10^3$ due to Eq. (8) neglecting the effect of unsaturated flow above water table (Marino, 1967; Tartakovsky and Neuman, 2007)." (lines 453 − 456 of the revised manuscript)

## References


Aguado, E., and Sitar, N.: Sensitivity analysis in aquifer studies, Water Resources Research, 13(4), 733−737, 1977.

An, H., Ichikawa, Y., Tachikawa, Y., and Shiiba, M.: Three-dimensional finite difference saturated-unsaturated flow modeling with nonorthogonal grids using a coordinate transformation method, Water Resour Res, 46, 2010.

An, H., Ichikawa, Y., Tachikawa, Y., and Shiiba, M.: Comparison between iteration schemes for three-dimensional coordinate-transformed saturated-unsaturated flow model, J Hydrol, 470, 212-226, 2012.

Cey, E., Rudolph, D., and Therrien, R.: Simulation of groundwater recharge dynamics in partially saturated fractured soils incorporating spatially variable fracture apertures, Water Resour Res, 42, 2006.

Chang, Y. C., and Yeh, H. D.: Analytical solution for groundwater flow in an anisotropic sloping aquifer with arbitrarily located multiwells, J Hydrol, 347, 143-152, 2007.

Dogan, A., and Motz, L. H.: Saturated-unsaturated 3D groundwater model. I: Development, J Hydrol Eng, 10, 492-504, 10.1061/(asce)1084-0699(2005)10:6(492), 2005.

Duffy, D. G.: Mixed boundary value problems, Chapman & Hall/CRC applied mathematics and nonlinear science series, Chapman & Hall/CRC Press, Boca Raton, 1, 2008.

Huang, Y.-C., and Yeh, H.-D.: Parameter identification for a slug test in a well with finite-thickness skin using extended Kalman filter, Water Resour Manage, 26(14), 4039-4057, 2012.

Hunt, R. J., Prudic, D. E., Walker, J. F., and Anderson, M. P.: Importance of unsaturated zone flow for simulating recharge in a humid climate, Ground Water, 46, 551-560, 10.1111/j.1745-6584.2007.00427.x, 2008.

Illas, T. S., Thomas, Z. S., and Andreas, P. C.: Water table fluctuation in aquifers overlying a semi-impervious layer due to transient recharge from a circular basin, J Hydrol, 348, 215-223, 2008.

Marino, M. A.: Hele-Shaw model study of the growth and decay of groundwater ridges, Journal of Geophysical Research, 72, 1195-1205, 10.1029/JZ072i004p01195, 1967.

Neuman, S. P.: Effect of partial penetration on flow in unconfined aquifers considering delayed gravity response, Water Resour Res, 10, 303-312, 10.1029/WR010i002p00303, 1974.

Neuman, S. P.: Analysis of pumping test data from anisotropic unconfined aquifers considering delayed gravity response, Water Resour Res, 11, 329-342, 10.1029/WR011i002p00329, 1975.

Rai, S. N., Ramana, D. V., and Singh, R. N.: On the prediction of ground-water mound formation in response to transient recharge from a circular basin, Water Resour Manag, 12, 271-284, 1998.

Rao, N. H., and Sarma, P. B. S.: Growth of groundwater mound in response to recharge, Ground Water, 18, 587-595, 1980.

Tartakovsky, G. D., and Neuman, S. P.: Three-dimensional saturated-unsaturated flow with axial symmetry to a partially penetrating well in a compressible unconfined aquifer, Water Resour Res, 43, 2007.

Yeh, H. D., Chen, Y. J.: Determination of skin and aquifer parameters for a slug test with wellbore-skin effect. J Hydro, 342(3–4), 283–294, 2007.

**Text abstracted from lines 203 − 256 and lines 473 − 531 of the revised manuscript**

The mathematical model, Eqs. (10) – (17b), can be solved by the methods of Laplace transform and double-integral transform. The former transform converts $\bar{h}(\bar{x},\bar{y},\bar{z},\bar{t})$ into $\tilde{h}(\bar{x},\bar{y},\bar{z},p)$, $\partial\bar{h}/\partial\bar{t}$ into $p\tilde{h}-\bar{h}|_{\bar{t}=0}$, and $\xi\bar{u}_x\bar{u}_y$ into $\xi\bar{u}_x\bar{u}_y/p$ where $p$ is the Laplace parameter and $\bar{h}|_{\bar{t}=0}$ equals zero in Eq. (11). After taking the transform, the model become a boundary value problem expressed as

$$\frac{\partial^2\tilde{h}}{\partial\bar{x}^2}+\kappa_y\frac{\partial^2\tilde{h}}{\partial\bar{y}^2}+\kappa_z\frac{\partial^2\tilde{h}}{\partial\bar{z}^2}=p\tilde{h} \tag{18}$$

with boundary conditions $\partial\tilde{h}/\partial\bar{x}-\kappa_1\tilde{h}=0$ at $\bar{x}=0$, $\partial\tilde{h}/\partial\bar{x}+\kappa_2\tilde{h}=0$ at $\bar{x}=\bar{l}$, $\tilde{h}/\partial\bar{y}-\kappa_3\tilde{h}=0$ at $\bar{y}=0$, $\tilde{h}/\partial\bar{y}+\kappa_4\tilde{h}=0$ at $\bar{y}=\bar{w}$, $\partial\tilde{h}/\partial\bar{z}=0$ at $\bar{z}=-1$, and $\partial\tilde{h}/\partial\bar{z}+\varepsilon p\tilde{h}/\kappa_z=\xi\bar{u}_x\bar{u}_y/p$ at $\bar{z}=0$. We then apply the properties of the double-integral transform to the problem. One can refer to the definition in Latinopoulos (1985, Table I, aquifer type 1). The transform turns $\tilde{h}(\bar{x},\bar{y},\bar{z},p)$ into $\hat{h}(\alpha_m,\beta_n,\bar{z},p)$, $\partial^2\tilde{h}/\partial\bar{x}^2+\kappa_y(\partial^2\tilde{h}/\partial\bar{y}^2)$ into $-(\alpha_m^2+\kappa_y\beta_n^2)\hat{h}$ where $(m, n) \in 1, 2, 3, \ldots \infty$, and eigenvalues $\alpha_m$ and $\beta_n$ are the positive roots of the following equations that

$$\tan(\bar{l}\alpha_m) = \frac{\alpha_m(\kappa_1+\kappa_2)}{\alpha_m^2-\kappa_1\kappa_2} \tag{19}$$

and

$$\tan(\bar{w}\beta_n) = \frac{\beta_n(\kappa_3+\kappa_4)}{\beta_n^2-\kappa_3\kappa_4}. \tag{20}$$

In addition, $\bar{u}_x\bar{u}_y$ defined in Eqs. (17a) and (17b) is transformed into $U_mU_n$ given by

$$U_m = \frac{\sqrt{2}V_m}{\sqrt{\kappa_1+(\alpha_m^2+\kappa_1^2)[\bar{l}+\kappa_2/(\alpha_m^2+\kappa_2^2)]}} \tag{21}$$

$$U_n = \frac{\sqrt{2}V_n}{\sqrt{\kappa_3+(\beta_n^2+\kappa_3^2)[\bar{w}+\kappa_4/(\beta_n^2+\kappa_4^2)]}} \tag{22}$$

with

$$V_m = \{\kappa_1[\cos(\alpha_m\bar{x}_1) - \cos(\alpha_m\chi)] - \alpha_m[\sin(\alpha_m\bar{x}_1) - \sin(\alpha_m\chi)]\}/\alpha_m \tag{23}$$

$$V_n = \{\kappa_3[\cos(\beta_n\bar{y}_1) - \cos(\beta_n\psi)] - \beta_n[\sin(\beta_n\bar{y}_1) - \sin(\beta_n\psi)]\}/\beta_n \tag{24}$$

where $\chi = \bar{x}_1 + \bar{a}$ and $\psi = \bar{y}_1 + \bar{b}$.

Equation (18) then reduces to an ordinary differential equation as

$$\kappa_z\frac{\partial^2\hat{h}}{\partial\bar{z}^2} - (p + \alpha_m^2 + \kappa_y\beta_n^2)\hat{h} = 0 \tag{25}$$

Two boundary conditions are expressed, respectively, as

$$\partial\hat{h}/\partial\bar{z} = 0 \quad \text{at} \quad \bar{z} = -1 \tag{26}$$

and

$$\frac{\partial\hat{h}}{\partial\bar{z}} + \frac{\varepsilon p}{\kappa_z}\hat{h} = \frac{\xi}{p}U_mU_n \quad \text{at} \quad \bar{z} = 0. \tag{27}$$

Solving Eq. (25) with Eqs. (26) and (27) results in

$$\hat{h}(\alpha_m, \beta_n, \bar{z}, p) = \frac{\xi U_mU_n\cosh[(1+\bar{z})\lambda]}{p(p\varepsilon\kappa_z\cosh\lambda+\kappa_z\lambda\sinh\lambda)} \tag{28}$$

where

$$\lambda = \sqrt{(p + \alpha_m^2 + \kappa_y\beta_n^2)/\kappa_z}. \tag{29}$$

Inverting Eq. (28) to the space and time domains gives rise to the analytical solution that

$$\bar{h}(\bar{x},\bar{y},\bar{z},\bar{t}) = \xi\sum_{m=1}^{\infty}\sum_{n=1}^{\infty}(\phi_{m,n} + \phi_{0,m,n} + \sum_{j=1}^{\infty}\phi_{j,m,n})F_mF_nU_mU_n \tag{30}$$

with

$$\phi_{m,n} = \frac{\cosh[(1+\bar{z})\lambda_{m,n}]}{\kappa_z\lambda_{m,n}\sinh\lambda_{m,n}} \tag{30a}$$

$$\phi_{0,m,n} = -2\lambda_{0,m,n}\cosh[(1+\bar{z})\lambda_{0,m,n}]\exp(-\gamma_{0,m,n}\bar{t})/\eta_{0,m,n} \tag{30b}$$

$$\phi_{j,m,n} = -2\lambda_{j,m,n}\cos[(1+\bar{z})\lambda_{j,m,n}]\exp(-\gamma_{j,m,n}\bar{t})/\eta_{j,m,n} \tag{30c}$$

$$\eta_{0,m,n} = \gamma_{0,m,n}[(1+2\varepsilon\kappa_z)\lambda_{0,m,n}\cosh\lambda_{0,m,n} + (1-\varepsilon\gamma_{0,m,n})\sinh\lambda_{0,m,n}] \tag{30d}$$

$$\eta_{j,m,n} = \gamma_{j,m,n}[(1+2\varepsilon\kappa_z)\lambda_{j,m,n}\cos\lambda_{j,m,n} + (1-\varepsilon\gamma_{j,m,n})\sin\lambda_{j,m,n}] \tag{30e}$$

$$\lambda_{m,n} = \sqrt{f_{m,n}/\kappa_z};\ \gamma_{0,m,n} = f_{m,n} - \kappa_z\lambda_{0,m,n}^2;\ \gamma_{j,m,n} = f_{m,n} + \kappa_z\lambda_{j,m,n}^2 \tag{30f}$$

$$f_{m,n} = \alpha_m^2 + \kappa_y\beta_n^2 \tag{30g}$$

$$F_m = \frac{\sqrt{2}[\alpha_m\cos(\alpha_m\bar{x}) + \kappa_1\sin(\alpha_m\bar{x})]}{\sqrt{\kappa_1 + (\alpha_m^2+\kappa_1^2)[\bar{l} + \kappa_2/(\alpha_m^2+\kappa_2^2)]}} \tag{30h}$$

$$F_n = \frac{\sqrt{2}[\beta_n\cos(\beta_n\bar{y}) + \kappa_3\sin(\beta_n\bar{y})]}{\sqrt{\kappa_3 + (\beta_n^2+\kappa_3^2)[\bar{w} + \kappa_4/(\beta_n^2+\kappa_4^2)]}} \tag{30i}$$

where $j \in 1, 2, 3, \ldots \infty$ and eigenvalues $\lambda_{0,m,n}$ and $\lambda_{j,m,n}$ are determined, respectively, by the following equations that

$$\tan\lambda_{j,m,n} = -\varepsilon(f_{m,n} + \kappa_z\lambda_{j,m,n}^2)/\lambda_{j,m,n} \tag{31}$$

and

$$\frac{-\varepsilon\kappa_z\lambda_{0,m,n}^2 + \lambda_{0,m,n} + \varepsilon f_{m,n}}{\varepsilon\kappa_z\lambda_{0,m,n}^2 + \lambda_{0,m,n} - \varepsilon f_{m,n}} = \exp(2\lambda_{0,m,n}). \tag{32}$$

Notice that Eqs. (19), (20), and (31) have infinite positive roots owing to the trigonometric function tan( ) while Eq. (32) has only one positive root. The method to find $\alpha_m$, $\beta_n$, $\lambda_{j,m,n}$ and $\lambda_{0,m,n}$ is introduced in Sect. 2.3. One can refer to Appendix A for the derivation of Eq. (30).

## Appendix A: Derivation of Eq. (30)

Let us start with function $G(p)$ from Eq. (28) that

$$G(p) = \frac{\cosh[(1+\bar{z})\lambda]}{p(p\varepsilon\kappa_z\cosh\lambda + \kappa_z\lambda\sinh\lambda)} \tag{A1}$$

with

$$\lambda = \sqrt{(p + f_{m,n})/\kappa_z} \tag{A2}$$

where $f_{m,n} = \alpha_m^2 + \kappa_y\beta_n^2$. Equation (A1) is a single-value function to $p$ in the complex plane because satisfying $G(p^+) = G(p^-)$ where $p^+$ and $p^-$ are the polar coordinates defined, respectively, as

$$p^+ = r_a\exp(i\theta) - f_{m,n} \tag{A3}$$

and

$$p^- = r_a\exp[i(\theta - 2\pi)] - f_{m,n} \tag{A4}$$

where $r_a$ represents a radial distance from the origin at $p = -f_{m,n}$, $i = \sqrt{-1}$ is the imaginary unit, and $\theta$ is an argument between 0 and $2\pi$. Substitute $p = p^+$ in Eq. (A3) into Eq. (A2), and we have

$$\lambda = \sqrt{r_a/\kappa_z}\exp(i\theta/2) = \sqrt{r_a/\kappa_z}\,[\cos(\theta/2) + i\sin(\theta/2)] \tag{A5}$$

Similarly, we can have

$$\lambda = \sqrt{r_a/\kappa_z}\exp[i(\theta - 2\pi)/2] = -\sqrt{r_a/\kappa_z}\,[\cos(\theta/2) + i\sin(\theta/2)] \tag{A6}$$

after $p$ in Eq. (A2) is replaced by $p^-$ in Eq. (A4). Substitution of Eqs. (A3) and (A5) into Eq. (A1) yields the same result as that obtained by substituting Eqs. (A4) and (A6) into Eq. (A1), indicating that Eq. (A1) is a single-value function without branch cut and its inverse Laplace transform equals the sum of residues for poles in the complex plane.

The residue for a simple pole can be formulated as

$$Res = \lim_{p\to\varphi} G(p)\exp(p\bar{t})\,(p - \varphi) \tag{A7}$$

where $\varphi$ is the location of the pole of $G(p)$ in Eq. (A1). The function $G(p)$ has infinite simple poles at the negative part of the real axis in the complex plane. The locations of these poles are the roots of equation that

$$p(p\varepsilon\kappa_z\cosh\lambda + \kappa_z\lambda\sinh\lambda) = 0 \tag{A8}$$

which is obtained by letting the denominator in Eq. (A1) to be zero. Obviously, one pole is at $p = 0$, and its residue based on Eqs. (A1) and (A7) with $\lambda_{m,n} = \sqrt{f_{m,n}/\kappa_z}$ can be expressed as

$$\phi_{m,n} = \cosh\big[(1 + \bar{z})\lambda_{m,n}\big]/(\kappa_z\lambda_{m,n}\sinh\lambda_{m,n}) \tag{A9}$$

The locations of other poles of $G(p)$ are the roots of the equation that

$$p\varepsilon\kappa_z\cosh\lambda + \kappa_z\lambda\sinh\lambda = 0 \tag{A10}$$

which is the expression in the parentheses in Eq. (A8). One pole is between $p = 0$ and $p = -f_{m,n}$. Let $\lambda = \lambda_{0,m,n}$, and Eq. (A2) becomes $p = -f_{m,n} + \kappa_z\lambda_{0,m,n}^2$. Substituting $\lambda = \lambda_{0,m,n}$, $p = -f_{m,n} + \kappa_z\lambda_{0,m,n}^2$, $\cosh\lambda_{0,m,n} = [\exp\lambda_{0,m,n} + \exp(-\lambda_{0,m,n})]/2$ and $\sinh\lambda_{0,m,n} = \big[\exp\lambda_{0,m,n} - \exp(-\lambda_{0,m,n})\big]/2$ into Eq. (A9) and rearranging the result lead to Eq. (32). The pole is at $p = -f_{m,n} + \kappa_z\lambda_{0,m,n}^2$ with a numerical value of $\lambda_{0,m,n}$. With Eq. (A1), Eq. (A7) equals

$$Res = \lim_{p\to\varphi}\frac{\cosh[(1+\bar{z})\lambda]}{p(p\varepsilon\kappa_z\cosh\lambda + \kappa_z\lambda\sinh\lambda)}\exp(p\bar{t})\,(p - \varphi) \tag{A11}$$

Apply L'Hospital's Rule to Eq. (A11), and then we have

$$Res = \lim_{p\to\varphi}\frac{-2\lambda\cosh[(1+\bar{z})\lambda]}{p[(1+2\varepsilon\kappa_z)\lambda\cosh\lambda + (1-\varepsilon p)\sinh\lambda]}\exp(p\bar{t}) \tag{A12}$$

The residue for the pole at $p = -f_{m,n} + \kappa_z\lambda_{0,m,n}^2$ can be defined as

$$\phi_{0,m,n} = \frac{-2\lambda_{0,m,n}\cosh[(1+\bar{z})\lambda_{0,m,n}]\exp(-\gamma_{0,m,n}\bar{t})}{\gamma_{0,m,n}[(1+2\varepsilon\kappa_z)\lambda_{0,m,n}\cosh\lambda_{0,m,n} + (1-\varepsilon\gamma_{0,m,n})\sinh\lambda_{0,m,n}]} \tag{A13}$$

which is obtained by Eq. (A12) with $\lambda = \lambda_{0,m,n}$ and $p = -f_{m,n} + \kappa_z \lambda_{0,m,n}^2 = \gamma_{0,m,n}$. On the other hand, infinite poles behind $p = -f_{m,n}$ are at $p = \gamma_{j,m,n}$ where $j \in 1, 2, 3, \ldots \infty$. Let $\lambda = \sqrt{-1}\lambda_{j,m,n}$, and Eq. (A2) yields $p = -f_{m,n} - \kappa_z \lambda_{j,m,n}^2$. Substituting $\lambda = \sqrt{-1}\lambda_{j,m,n}$, $p = -f_{m,n} - \kappa_z \lambda_{j,m,n}^2$, $\cosh\left(\sqrt{-1}\lambda_{j,m,n}\right) = \cos \lambda_{j,m,n}$, and $\sinh\left(\sqrt{-1}\lambda_{j,m,n}\right) = \sqrt{-1} \sin\lambda_{j,m,n}$ into Eq. (A9) and rearranging the result gives rise to Eq. (31). These poles are at $p = -f_{m,n} - \kappa_z \lambda_{j,m,n}^2$ with numerical values of $\lambda_{j,m,n}$. On the basis of Eq. (A12) with $\lambda = \sqrt{-1}\lambda_{j,m,n}$ and $p = -f_{m,n} - \kappa_z \lambda_{j,m,n}^2 = \gamma_{j,m,n}$, the residues for these poles at $p = -f_{m,n} - \kappa_z \lambda_{j,m,n}^2$ can be expressed as

$$\phi_{j,m,n} = \frac{-2\lambda_{j,m,n} \cos[(1+\bar{z})\lambda_{j,m,n}] \exp(-\gamma_{j,m,n}\bar{t})}{\gamma_{j,m,n}[(1+2\varepsilon\kappa_z)\lambda_{j,m,n} \cos\lambda_{j,m,n} + (1-\varepsilon\gamma_{j,m,n}) \sin\lambda_{j,m,n}]} \tag{A14}$$

As a result, the inverse Laplace transform for Eq. (A1) is the sum of Eqs. (A9) and (A13) and a simple series expended in the RHS function in Eq. (A14) (i.e., $\phi_{m,n} + \phi_{0,m,n} + \sum_{j=1}^{\infty} \phi_{j,m,n}$). Finally, Eq. (30) can be derived after taking the inverse double-integral transform for the result using the formula that (Latinopoulos, 1985, Eq. (14))

$$\bar{h}(\bar{x}, \bar{y}, \bar{z}, \bar{t}) = \xi \sum_{m=1}^{\infty} \sum_{n=1}^{\infty} \left(\phi_{m,n} + \phi_{0,m,n} + \sum_{j=1}^{\infty} \phi_{j,m,n}\right) F_m F_n U_m U_n \tag{A15}$$

where $\xi$ and $U_m U_n$ result from $\xi U_m U_n$ in Eq. (28).

# Responses to 1st Comment of Referee #2

## 1 General comments

The authors have treated a difficult and complicated hydrological problem. The solution methods are of a standard mathematical nature, but by no means trivial. Their final solution becomes a triple sum where zeros of transcedental equations have to be calculated. Moreover, the factors for the horizontal contributions $F_x(\alpha_m,\ \bar{x})$ and $F_y(\beta_n,\ \bar{y})$ are independent, but the term $\Phi(\alpha_m, \beta_n,\ \bar{z},\ \bar{t})$ depends on $\alpha_m$ and $\beta_n$ by means of the variable $f = \alpha_m^2 + \kappa_z \beta_m^2$. This analytical solution belongs to Class 2 according the classification in Veling and Maas (2009).

The style of the paper is straightforward and the derivation in the Appendix is intelligible.

In their sensitivity analysis the authors give useful dimensionless expressions with criteria when to use which approximation for given circumstances and when an approximation is not appropriate. Their sensitivity analysis could be extended even further by treating the boundary conditions in a different way.

The authors do not give much information about the numerical evaluation of the found analytical expression other than some details how the zeros of the transcedental equations have been found. A validation of solution has not been supplied other than comparisons with other published solutions of simpler problems. It is possible to make choices for the parameters such that this solution should be equal to earlier published ones (*e.g.* the recharge area is the whole aquifer). In that way an independent, partial check of this solution could be possible.

Can the authors give information about the performance of their code (calculation times, convergence properties of the triple sums) and about the availability?

The general impression is a good piece of technical work based on well-established equations and boundary conditions for such cases. This solution based on the inclusion of equation (8) (time dependent first order free surface equation) for the chosen finite aquifer with a finite recharge domain seems to be new.

Response: Thanks for the comment. It is indeed an interesting work to reduce the present solution to earlier published ones or to show their equivalency/equality. To the best of our knowledge, there have been four existing analytical solutions dealing with similar topics to this note (Zlotnik and Ledder, 1993; Ramana et al., 1995; Manglik et al., 1997; Manglik and Rai, 1998). Unfortunately, our solution cannot reduce to the Zlotnik and Ledder (1993) solution because their solution is based on aquifers of infinite extent in the horizontal direction while ours considers aquifers of finite extent. Neither, the present solution cannot reduce to any of the other three solutions due to different mathematical representations of regional recharge. Those solutions regard recharge as a source term in two-dimensional flow equation and are thus independent of elevation *z*. On the other hand, our solution considers regional recharge as a boundary condition specified on the top of the aquifer (Please refer to Yeh and Yeh (2007) for discussing the differences in point-source and boundary-source solutions), triggering the vertical flow below the recharge area and making the flow field three dimensional. Nevertheless, the present solution and those four solutions can give the same hydraulic head prediction at observation points under certain conditions discussed in sections 3.1 − 3.4 in the previous manuscript.

We add following text in the revised manuscript to address convergence of the series in the present solution:

"The first term on the right-hand side (RHS) of Eq. (30) is a double series expanded by $\alpha_m$ and $\beta_n$. The series converges within a few terms because the power of $\alpha_m$ (or $\beta_n$) in the denominator of $\phi_{m,n}$ in Eq. (30a) is two more than that in the nominator. The second term on the RHS of Eq. (30) is a double series expanded by $\alpha_m$ and $\beta_n$, and the third term is a triple series expanded by $\alpha_m$, $\beta_n$, and $\lambda_{j,m,n}$. They converge very fast due to exponential functions in Eqs. (30b) and (30c). Consider $(m, n) \in (1, 2, \ldots, N = 30)$ and $j \in (1, 2, \ldots, N_j = 15)$ for the default values of dimensionless parameters and variables in Table 2 for calculation. The number of terms in one or the other double series is 30 × 30 = 900 and in the triple series is 30 × 30 × 15 = 13500. The total number is therefore 900 × 2 + 13500 = 15300. We apply Mathematica FindRoot routine to obtain the values of $\alpha_m$, $\beta_n$, and $\lambda_{j,m,n}$ and Sum routine to compute the double and triple series. It takes about 8 seconds to finish calculation for $\bar{t} = 10^5$ by a personal computer with Intel Core i5-4590 3.30 GHz processor and 8 GB RAM. In addition, the series is considered to converge when the absolute value of the last term in the double series of $\phi_{m,n}$ is smaller than $10^{-20}$ (i.e., $10^{-50} < 10^{-20}$ in this case). That value in the other double or triple series may be even smaller than $10^{-50}$ due to exponential decay." (lines 256 − 270 of the revised manuscript)

At the end of Acknowledgements, we add the sentence "The computer software used to generate the results in Figures 2−6 is available upon request."

## 2 Some specific remarks

Page 12249, l. 9: No mention is made of the work of Bruggeman (1999, 360 BIII-6, from p. 321) for comparable solutions in a finite strip.

Response: Thanks, we insert the following sentence in the revised manuscript:

"Bruggeman (1999) introduced an analytical solution for steady-state flow induced by localized recharge into a vertical strip aquifer between two Robin boundaries." (lines 79 − 80 of the revised manuscript)

Page 12252, l. 24: The introduction of the distance d is unclear in the case that the location of the observation well has coordinates ($x_w$, $y_w$) with $x_w > x_1 + a$, $y_w > y_1 + b$ or $x_w > x_1 + a$, $y_w < y_1$ or $x_w < x_1$, $y_w > y_1 + b$ or $x_w < x_1$, $y_w < y_1$. What should be the distance in such cases:

$$\mathrm{d} = \min(|x_w - x - a|, |y_w - y_1 - b|, |x_w - x_1|, |y_w - y_1|)$$

or

$$\mathrm{d} = \min\left(\begin{array}{c}\sqrt{\left(x_w - (x_1 + a)\right)^2 + \left(y_w - (y_1 + b)\right)^2}, \sqrt{\left(x_w - (x_1 + a)\right)^2 + (y_w - y_1)^2}, \\ \sqrt{(x_w - x_1)^2 + (y_w - (y_1 + b))^2}, \sqrt{(x_w - x_1)^2 + (y_w - y_1)^2}\end{array}\right) ?$$

Response: Thanks for the comment. Following sentence is added to give an explicit definition of *d* in the revised manuscript:

"The shortest distance between the edge of the region and an observation point at $(x, y)$ is defined as $d = \min(\sqrt{(x - x_e)^2 + (y - y_e)^2})$ where $(x_e, y_e)$ is a coordinate on the edge." (lines 144 − 146 of the revised manuscript)

Page 12254, l. 4: The symbol l for the recharge rate has been introduced earlier for the width in the *x*-direction of the rectangular aquifer.

Response: Thanks, this is a typo by the typesetter of this journal. We will correct it.

Page 12254: l. 12: Remark the way of scaling: with d in the horizontal plane and with B in the vertical plane.

Response: We inserted the following sentence after the dimensionless definitions in equation (9):

"Notice that the variables in the horizontal and vertical directions are divided by *d* and *B*, respectively." (lines 188 − 189 of the revised manuscript)

Page 12257, l. 1: It should be better to label f as $f_{m, n}$ to make clear the dependency on $\alpha_m$ and $\beta_n$. In fact, also $\lambda_j$ should be better $\lambda_{j, m, n}$. In the current presentation the solution looks simpler that it is really!

Response: Thanks, they have been changed as suggested. Please refer to the new expression of the present solution at the end of this reply.

Page 12258, l. 20: More explanation is needed for formula (23); specify a reference here for the use of Duhamel's Principle. Very likely, in the denominator $\xi$ should be $\xi_t(0)$.

Response: We added the reference "Singh (2005)". It is $1/\xi$ rather than $1/\xi_t(0)$ so that coefficient $\xi$ in equation (30) at the end of this reply can be eliminated.

Page 12258, after Section 3.2: Some information could be given about the way the authors have treated the triple sum numerically. Did they use convergence accelerators?

Response: No, we did not use accelerators because the present solution converges very fast (i.e., only a few terms are needed to achieve good accuracy). Please refer to the first response for the discussion on series convergence.

Page 12261, l. 5: The mention of "Fig. 2" does not seem to be correct.

Response: Thanks for the comment. It has been deleted.

Page 12264, l. 18: The sensitivity analysis w.r.t. *a*: have the authors taken in consideration that by changing *a* also the scaling variable *d* changes too by the chosen location of the observation points/wells A and B?

Response: Variable *d* equals a fixed value of 5 m for the case of observation point A and 250 m for the case of observation point B in Figure 6 in the manuscript.

## 3 Some minor remarks

Page 12248, l. 24: Change "the" into "a".

Response: As suggested.

Page 12257, l. 1, formula (18o): It is more natural to introduce variables before and not after the introduction of the formulas where they are used explicitly. The same applies to formulas (18k) and (18m). As exhibited here in this paper the distance between use and definition is rather great.

Response: Thanks for the comment. The order of these equations are rearranged. The associated text is given at the end of this reply.

Page 12257, l. 11: Change "first and second" into " second and third".

Page 12257, l. 12: Change "third" into "first".

Response: The associated text is revised according to new arrangement of equations.

Page 12260, l. 7: Very likely, the authors mean $10^{-3}P_c$ in stead of $10^{-3}\Delta P_c$.

Page 12264, l. 10: Change "squire" into "square".

Page 12271:, l. 3: Change "cauchy" into "Cauchy".

Responses: We thank reviewer's eyes in detail. They have been revised as suggested.

## 4 References

## References

G. A. Bruggeman. *Analytical Solutions of Geohydrological Problems*. Developments in Water Science, nr. 46. Elsevier, Amsterdam, 1999.

E. J. M. Veling and C. Maas. Strategy for solving semi-analytically three-dimensional transient .ow in a coupled N-layer aquifer system. *Journal of Engineering Mathematics*, 64(2):145–161, doi:10.1007/s10665.008.9256.9, 2009.

**References**

Bruggeman, G. A.: Analytical Solutions of Geohydrological Problems, Elsevier, Netherlands, 326, 1999.

Manglik, A., Rai, S. N., and Singh, R. N.: Response of an Unconfined Aquifer Induced by Time Varying Recharge from a Rectangular Basin, Water Resour Manag, 11, 185-196, 1997.

Manglik, A., and Rai, S. N.: Two-Dimensional Modelling of Water Table Fluctuations due to Time-Varying Recharge from Rectangular Basin, Water Resour Manag, 12, 467-475, 1998.

Ramana, D. V., Rai, S. N., and Singh, R. N.: Water table fluctuation due to transient recharge in a 2-D aquifer system with inclined base, Water Resour Manag, 9, 127-138, 10.1007/BF00872464, 1995.

Singh, S. K.: Rate and volume of stream flow depletion due to unsteady pumping, J Irrig Drain E-Asce, 131, 539-545, 2005.

Yeh, H. D., and Yeh, G. T.: Analysis of point-source and boundary-source solutions of one-dimensional groundwater transport equation, J Environ Eng-Asce, 133, 1032-1041, 2007.

Zlotnik, V., and Ledder, G.: Groundwater velocity in an unconfined aquifer with rectangular areal recharge, Water Resour Res, 29, 2827-2834, 1993.

**Text abstracted from lines 203 − 256 and lines 473 − 531 of the revised manuscript**

The mathematical model, Eqs. (10) – (17b), can be solved by the methods of Laplace transform and double-integral transform. The former transform converts $\bar{h}(\bar{x},\bar{y},\bar{z},\bar{t})$ into $\tilde{h}(\bar{x},\bar{y},\bar{z},p)$, $\partial\bar{h}/\partial\bar{t}$ into $p\tilde{h}-\bar{h}|_{\bar{t}=0}$, and $\xi\bar{u}_x\bar{u}_y$ into $\xi\bar{u}_x\bar{u}_y/p$ where $p$ is the Laplace parameter and $\bar{h}|_{\bar{t}=0}$ equals zero in Eq. (11). After taking the transform, the model become a boundary value problem expressed as

$$\frac{\partial^2\tilde{h}}{\partial\bar{x}^2}+\kappa_y\frac{\partial^2\tilde{h}}{\partial\bar{y}^2}+\kappa_z\frac{\partial^2\tilde{h}}{\partial\bar{z}^2}=p\tilde{h} \tag{18}$$

with boundary conditions $\partial\tilde{h}/\partial\bar{x}-\kappa_1\tilde{h}=0$ at $\bar{x}=0$, $\partial\tilde{h}/\partial\bar{x}+\kappa_2\tilde{h}=0$ at $\bar{x}=\bar{l}$, $\tilde{h}/\partial\bar{y}-\kappa_3\tilde{h}=0$ at $\bar{y}=0$, $\tilde{h}/\partial\bar{y}+\kappa_4\tilde{h}=0$ at $\bar{y}=\bar{w}$, $\partial\tilde{h}/\partial\bar{z}=0$ at $\bar{z}=-1$, and $\partial\tilde{h}/\partial\bar{z}+\varepsilon p\tilde{h}/\kappa_z=\xi\bar{u}_x\bar{u}_y/p$ at $\bar{z}=0$. We then apply the properties of the double-integral transform to the problem. One can refer to the definition in Latinopoulos (1985, Table I, aquifer type 1). The transform turns $\tilde{h}(\bar{x},\bar{y},\bar{z},p)$ into $\hat{h}(\alpha_m,\beta_n,\bar{z},p)$, $\partial^2\tilde{h}/\partial\bar{x}^2+\kappa_y(\partial^2\tilde{h}/\partial\bar{y}^2)$ into $-(\alpha_m^2+\kappa_y\beta_n^2)\hat{h}$ where $(m, n) \in 1, 2, 3, \ldots \infty$, and eigenvalues $\alpha_m$ and $\beta_n$ are the positive roots of the following equations that

$$\tan(\bar{l}\alpha_m)=\frac{\alpha_m(\kappa_1+\kappa_2)}{\alpha_m^2-\kappa_1\kappa_2} \tag{19}$$

and

$$\tan(\bar{w}\beta_n)=\frac{\beta_n(\kappa_3+\kappa_4)}{\beta_n^2-\kappa_3\kappa_4}. \tag{20}$$

In addition, $\bar{u}_x\bar{u}_y$ defined in Eqs. (17a) and (17b) is transformed into $U_mU_n$ given by

$$U_m=\frac{\sqrt{2}V_m}{\sqrt{\kappa_1+(\alpha_m^2+\kappa_1^2)[\bar{l}+\kappa_2/(\alpha_m^2+\kappa_2^2)]}} \tag{21}$$

$$U_n=\frac{\sqrt{2}V_n}{\sqrt{\kappa_3+(\beta_n^2+\kappa_3^2)[\bar{w}+\kappa_4/(\beta_n^2+\kappa_4^2)]}} \tag{22}$$

with

$$V_m=\{\kappa_1[\cos(\alpha_m\bar{x}_1)-\cos(\alpha_m\chi)]-\alpha_m[\sin(\alpha_m\bar{x}_1)-\sin(\alpha_m\chi)]\}/\alpha_m \tag{23}$$

$$V_n=\{\kappa_3[\cos(\beta_n\bar{y}_1)-\cos(\beta_n\psi)]-\beta_n[\sin(\beta_n\bar{y}_1)-\sin(\beta_n\psi)]\}/\beta_n \tag{24}$$

where $\chi=\bar{x}_1+\bar{a}$ and $\psi=\bar{y}_1+\bar{b}$.

Equation (18) then reduces to an ordinary differential equation as

$$\kappa_z\frac{\partial^2\hat{h}}{\partial\bar{z}^2}-(p+\alpha_m^2+\kappa_y\beta_n^2)\hat{h}=0 \tag{25}$$

Two boundary conditions are expressed, respectively, as

$$\partial\hat{h}/\partial\bar{z}=0 \quad \text{at} \quad \bar{z}=-1 \tag{26}$$

and

$$\frac{\partial \hat{h}}{\partial \bar{z}} + \frac{\varepsilon p}{\kappa_z}\hat{h} = \frac{\xi}{p} U_m U_n \quad \text{at} \quad \bar{z} = 0. \tag{27}$$

Solving Eq. (25) with Eqs. (26) and (27) results in

$$\hat{h}(\alpha_m, \beta_n, \bar{z}, p) = \frac{\xi U_m U_n \cosh[(1+\bar{z})\lambda]}{p(p\varepsilon\kappa_z \cosh\lambda + \kappa_z \lambda \sinh\lambda)} \tag{28}$$

where

$$\lambda = \sqrt{(p + \alpha_m^2 + \kappa_y \beta_n^2)/\kappa_z}. \tag{29}$$

Inverting Eq. (28) to the space and time domains gives rise to the analytical solution that

$$\bar{h}(\bar{x}, \bar{y}, \bar{z}, \bar{t}) = \xi \sum_{m=1}^{\infty} \sum_{n=1}^{\infty} (\phi_{m,n} + \phi_{0,m,n} + \sum_{j=1}^{\infty} \phi_{j,m,n}) F_m F_n U_m U_n \tag{30}$$

with

$$\phi_{m,n} = \frac{\cosh[(1+\bar{z})\lambda_{m,n}]}{\kappa_z \lambda_{m,n} \sinh\lambda_{m,n}} \tag{30a}$$

$$\phi_{0,m,n} = -2\lambda_{0,m,n} \cosh[(1+\bar{z})\lambda_{0,m,n}] \exp(-\gamma_{0,m,n}\bar{t})/\eta_{0,m,n} \tag{30b}$$

$$\phi_{j,m,n} = -2\lambda_{j,m,n} \cos[(1+\bar{z})\lambda_{j,m,n}] \exp(-\gamma_{j,m,n}\bar{t})/\eta_{j,m,n} \tag{30c}$$

$$\eta_{0,m,n} = \gamma_{0,m,n}[(1+2\varepsilon\kappa_z)\lambda_{0,m,n} \cosh\lambda_{0,m,n} + \left(1-\varepsilon\gamma_{0,m,n}\right)\sinh\lambda_{0,m,n}] \tag{30d}$$

$$\eta_{j,m,n} = \gamma_{j,m,n}[(1+2\varepsilon\kappa_z)\lambda_{j,m,n} \cos\lambda_{j,m,n} + \left(1-\varepsilon\gamma_{j,m,n}\right)\sin\lambda_{j,m,n}] \tag{30e}$$

$$\lambda_{m,n} = \sqrt{f_{m,n}/\kappa_z};\ \gamma_{0,m,n} = f_{m,n} - \kappa_z \lambda_{0,m,n}^2;\ \gamma_{j,m,n} = f_{m,n} + \kappa_z \lambda_{j,m,n}^2 \tag{30f}$$

$$f_{m,n} = \alpha_m^2 + \kappa_y \beta_n^2 \tag{30g}$$

$$F_m = \frac{\sqrt{2}[\alpha_m \cos(\alpha_m \bar{x}) + \kappa_1 \sin(\alpha_m \bar{x})]}{\sqrt{\kappa_1 + (\alpha_m^2 + \kappa_1^2)[\bar{l} + \kappa_2/(\alpha_m^2 + \kappa_2^2)]}} \tag{30h}$$

$$F_n = \frac{\sqrt{2}[\beta_n \cos(\beta_n \bar{y}) + \kappa_3 \sin(\beta_n \bar{y})]}{\sqrt{\kappa_3 + (\beta_n^2 + \kappa_3^2)[\bar{w} + \kappa_4/(\beta_n^2 + \kappa_4^2)]}} \tag{30i}$$

where $j \in 1, 2, 3, \ldots \infty$ and eigenvalues $\lambda_{0,m,n}$ and $\lambda_{j,m,n}$ are determined, respectively, by the following equations that

$$\tan\lambda_{j,m,n} = -\varepsilon(f_{m,n} + \kappa_z \lambda_{j,m,n}^2)/\lambda_{j,m,n} \tag{31}$$

and

$$\frac{-\varepsilon\kappa_z\lambda_{0,m,n}^2 + \lambda_{0,m,n} + \varepsilon f_{m,n}}{\varepsilon\kappa_z\lambda_{0,m,n}^2 + \lambda_{0,m,n} - \varepsilon f_{m,n}} = \exp(2\lambda_{0,m,n}). \tag{32}$$

Notice that Eqs. (19), (20), and (31) have infinite positive roots owing to the trigonometric function tan( ) while Eq. (32) has only one positive root. The method to find $\alpha_m$, $\beta_n$, $\lambda_{j,m,n}$ and $\lambda_{0,m,n}$ is introduced in Sect. 2.3. One can refer to Appendix A for the derivation of Eq. (30).

## Appendix A: Derivation of Eq. (30)

Let us start with function $G(p)$ from Eq. (28) that

$$G(p) = \frac{\cosh[(1+\bar{z})\lambda]}{p(p\varepsilon\kappa_z \cosh\lambda + \kappa_z\lambda\sinh\lambda)} \tag{A1}$$

with

$$\lambda = \sqrt{(p + f_{m,n})/\kappa_z} \tag{A2}$$

where $f_{m,n} = \alpha_m^2 + \kappa_y\beta_n^2$. Equation (A1) is a single-value function to $p$ in the complex plane because satisfying $G(p^+) = G(p^-)$ where $p^+$ and $p^-$ are the polar coordinates defined, respectively, as

$$p^+ = r_a\exp(i\theta) - f_{m,n} \tag{A3}$$

and

$$p^- = r_a\exp[i(\theta - 2\pi)] - f_{m,n} \tag{A4}$$

where $r_a$ represents a radial distance from the origin at $p = -f_{m,n}$, $i = \sqrt{-1}$ is the imaginary unit, and $\theta$ is an argument between 0 and $2\pi$. Substitute $p = p^+$ in Eq. (A3) into Eq. (A2), and we have

$$\lambda = \sqrt{r_a/\kappa_z}\exp(i\theta/2) = \sqrt{r_a/\kappa_z}\,[\cos(\theta/2) + i\sin(\theta/2)] \tag{A5}$$

Similarly, we can have

$$\lambda = \sqrt{r_a/\kappa_z}\exp[i(\theta - 2\pi)/2] = -\sqrt{r_a/\kappa_z}\,[\cos(\theta/2) + i\sin(\theta/2)] \tag{A6}$$

after $p$ in Eq. (A2) is replaced by $p^-$ in Eq. (A4). Substitution of Eqs. (A3) and (A5) into Eq. (A1) yields the same result as that obtained by substituting Eqs. (A4) and (A6) into Eq. (A1), indicating that Eq. (A1) is a single-value function without branch cut and its inverse Laplace transform equals the sum of residues for poles in the complex plane.

The residue for a simple pole can be formulated as

$$Res = \lim_{p\to\varphi} G(p)\exp(p\bar{t})\,(p - \varphi) \tag{A7}$$

where $\varphi$ is the location of the pole of $G(p)$ in Eq. (A1). The function $G(p)$ has infinite simple poles at the negative part of the real axis in the complex plane. The locations of these poles are the roots of equation that

$$p(p\varepsilon\kappa_z\cosh\lambda + \kappa_z\lambda\sinh\lambda) = 0 \tag{A8}$$

which is obtained by letting the denominator in Eq. (A1) to be zero. Obviously, one pole is at $p = 0$, and its residue based on Eqs. (A1) and (A7) with $\lambda_{m,n} = \sqrt{f_{m,n}/\kappa_z}$ can be expressed as

$$\phi_{m,n} = \cosh\left[(1+\bar{z})\lambda_{m,n}\right]/(\kappa_z\lambda_{m,n}\sinh\lambda_{m,n}) \tag{A9}$$

The locations of other poles of $G(p)$ are the roots of the equation that

$$p\varepsilon\kappa_z \cosh\lambda + \kappa_z\lambda\sinh\lambda = 0 \tag{A10}$$

which is the expression in the parentheses in Eq. (A8). One pole is between $p = 0$ and $p = -f_{m,n}$. Let $\lambda = \lambda_{0,m,n}$, and Eq. (A2) becomes $p = -f_{m,n} + \kappa_z\lambda_{0,m,n}^2$. Substituting $\lambda = \lambda_{0,m,n}$, $p = -f_{m,n} + \kappa_z\lambda_{0,m,n}^2$, $\cosh\lambda_{0,m,n} = [\exp\lambda_{0,m,n} + \exp(-\lambda_{0,m,n})]/2$ and $\sinh\lambda_{0,m,n} = [\exp\lambda_{0,m,n} - \exp(-\lambda_{0,m,n})]/2$ into Eq. (A9) and rearranging the result lead to Eq. (32). The pole is at $p = -f_{m,n} + \kappa_z\lambda_{0,m,n}^2$ with a numerical value of $\lambda_{0,m,n}$. With Eq. (A1), Eq. (A7) equals

$$Res = \lim_{p\to\varphi} \frac{\cosh[(1+\bar{z})\lambda]}{p(p\varepsilon\kappa_z\cosh\lambda + \kappa_z\lambda\sinh\lambda)} \exp(p\bar{t})\,(p-\varphi) \tag{A11}$$

Apply L'Hospital's Rule to Eq. (A11), and then we have

$$Res = \lim_{p\to\varphi} \frac{-2\lambda\cosh[(1+\bar{z})\lambda]}{p[(1+2\varepsilon\kappa_z)\lambda\cosh\lambda + (1-\varepsilon p)\sinh\lambda]} \exp(p\bar{t}) \tag{A12}$$

The residue for the pole at $p = -f_{m,n} + \kappa_z\lambda_{0,m,n}^2$ can be defined as

$$\phi_{0,m,n} = \frac{-2\lambda_{0,m,n}\cosh[(1+\bar{z})\lambda_{0,m,n}]\exp(-\gamma_{0,m,n}\bar{t})}{\gamma_{0,m,n}[(1+2\varepsilon\kappa_z)\lambda_{0,m,n}\cosh\lambda_{0,m,n} + (1-\varepsilon\gamma_{0,m,n})\sinh\lambda_{0,m,n}]} \tag{A13}$$

which is obtained by Eq. (A12) with $\lambda = \lambda_{0,m,n}$ and $p = -f_{m,n} + \kappa_z\lambda_{0,m,n}^2 = \gamma_{0,m,n}$. On the other hand, infinite poles behind $p = -f_{m,n}$ are at $p = \gamma_{j,m,n}$ where $j \in 1, 2, 3, \ldots \infty$. Let $\lambda = \sqrt{-1}\lambda_{j,m,n}$, and Eq. (A2) yields $p = -f_{m,n} - \kappa_z\lambda_{j,m,n}^2$. Substituting $\lambda = \sqrt{-1}\lambda_{j,m,n}$, $p = -f_{m,n} - \kappa_z\lambda_{j,m,n}^2$, $\cosh(\sqrt{-1}\lambda_{j,m,n}) = \cos\lambda_{j,m,n}$, and $\sinh(\sqrt{-1}\lambda_{j,m,n}) = \sqrt{-1}\sin\lambda_{j,m,n}$ into Eq. (A9) and rearranging the result gives rise to Eq. (31). These poles are at $p = -f_{m,n} - \kappa_z\lambda_{j,m,n}^2$ with numerical values of $\lambda_{j,m,n}$. On the basis of Eq. (A12) with $\lambda = \sqrt{-1}\lambda_{j,m,n}$ and $p = -f_{m,n} - \kappa_z\lambda_{j,m,n}^2 = \gamma_{j,m,n}$, the residues for these poles at $p = -f_{m,n} - \kappa_z\lambda_{j,m,n}^2$ can be expressed as

$$\phi_{j,m,n} = \frac{-2\lambda_{j,m,n}\cos[(1+\bar{z})\lambda_{j,m,n}]\exp(-\gamma_{j,m,n}\bar{t})}{\gamma_{j,m,n}[(1+2\varepsilon\kappa_z)\lambda_{j,m,n}\cos\lambda_{j,m,n} + (1-\varepsilon\gamma_{j,m,n})\sin\lambda_{j,m,n}]} \tag{A14}$$

As a result, the inverse Laplace transform for Eq. (A1) is the sum of Eqs. (A9) and (A13) and a simple series expended in the RHS function in Eq. (A14) (i.e., $\phi_{m,n} + \phi_{0,m,n} + \sum_{j=1}^{\infty}\phi_{j,m,n}$). Finally, Eq. (30) can be derived after taking the inverse double-integral transform for the result using the formula that (Latinopoulos, 1985, Eq. (14))

$$\bar{h}(\bar{x},\bar{y},\bar{z},\bar{t}) = \xi\sum_{m=1}^{\infty}\sum_{n=1}^{\infty}(\phi_{m,n} + \phi_{0,m,n} + \sum_{j=1}^{\infty}\phi_{j,m,n})F_mF_nU_mU_n \tag{A15}$$

where $\xi$ and $U_mU_n$ result from $\xi U_mU_n$ in Eq. (28).

## Responses to 2nd Comment of Referee #2

## 1 General comments

The authors responded carefully to my earlier remarks.

One point remains. The reference they included w.r.t. formula (23) in the original manuscript (p. 12258) about the solution for time-varying recharge rate does not learn us more that just the same formula. It is advised to include a reference for the Duhamel Principle in a well-known book, e.g. Bear (1972, p. 300) or Bear (1979, formula (5-150)) (both without proof; from the presentation in these references the formula (23) can easily be derived by the method of Integration by Parts) or a reference with a mathematical proof (e.g. Sneddon (1986, p. 279-281) or Bartels and Churchill (1942)). The last reference uses the Laplace Transform technique.

Response: Thanks for the suggestion. The related sentence is rewritten as:

"The present solution, Eq. (30), is applicable to arbitrary time-depending recharge rates on the basis of Duhamel's theorem expressed as (e.g., Bear, 1979, p. 158)

$$\bar{h}_{It} = \bar{h}_{I0} + \int_0^{\bar{t}} \frac{\partial \xi_t(\tau)}{\partial \tau} \bar{h}(\bar{t} - \tau)/\xi \, d\tau \qquad (33)"$$

(lines 297 − 299 of the revised manuscript)

## 2 Some minor remark

Page 12272, l. 1: Change "Ralte" into "Rate".

Response: Many thanks, it has been corrected as suggested.

## References

R.C.F. Bartels and R.V. Churchill. Resolution of boundary problems by the use of a generalized convolution. Bulletin of the American Mathematical Society, 48:276—282, 1942.

J. Bear. Dynamics of Fluids in Porous Media. American Elsevier, New York, 1972.

Jacob Bear. Hydraulics of Groundwater. McGraw-Hill, New York, 1979.

Ian N. Sneddon. Elements of Partial Differential Equations. McGraw-Hill, New York, 1986.

**Reference**

Bear, J.: Hydraulics of Groundwater, McGraw-Hill, New York, 158, 1979.

# Technical Note: Three-dimensional transient groundwater flow due to localized recharge with an arbitrary transient rate in unconfined aquifers

**Chia-Hao Chang[1], Ching-Sheng Huang[1], and Hund-Der Yeh[1,*]**

Re-submitted to *Hydrology and Earth System Sciences* on Feb. 3, 2016

Manuscript number: hess-2015-402

[1] Institute of Environmental Engineering, National Chiao Tung University, Hsinchu, Taiwan

*** Corresponding Author**

Address: Institute of Environmental Engineering, National Chiao Tung University, 1001 University Road, Hsinchu 300, Taiwan

E-mail address: hdyeh@mail.nctu.edu.tw; Tel: 886-3-5731910; Fax: 886-3-5725958

**Abstract**

Most previous solutions for groundwater flow induced by localized recharge assumed either aquifer incompressibility or two-dimensional flow in the absence of the vertical flow. This paper develops a new three-dimensional flow model for hydraulic head variation due to localized recharge in a rectangular unconfined aquifer with four boundaries under the Robin condition. A governing equation describing spatiotemporal head distributions is employed. The first-order free surface equation with a source term defining a constant recharge rate over a rectangular area is used to depict water table movement. The solution of the model for the head is developed by the methods of Laplace transform and double integral transform. Based on Duhamel's theorem, the present solution is applicable to flow problems accounting for arbitrary time-depending recharge rates. The solution of depth-average head can then be obtained by integrating the head solution to elevation and dividing the result by the aquifer thickness. The use of rectangular aquifer domain has two merits. One is that the integration for estimating the depth-average head can be analytically achieved. The other is that existing solutions based on aquifers of infinite extent can be considered as special cases of the present solution before the time having the aquifer boundary effect on head predictions. With the help of the present solution, the assumption of neglecting the vertical flow effect on the temporal head distribution at an observation point outside a recharge region can be assessed by a dimensionless parameter related to the aquifer horizontal and vertical hydraulic conductivities, initial aquifer thickness, and a shortest distance between the observation point and the edge of the recharge region. The validity of assuming aquifer incompressibility is dominated by the ratio of the aquifer specific yield to its storage coefficient. In addition, a sensitivity analysis is performed to investigate the head response to the change in each of the aquifer parameters.

**Keywords:** analytical solution, free surface equation, sensitivity analysis, localized recharge, unconfined aquifers.

## 1 Introduction

Water table rises due to localized recharge such as rainfall, lakes, and agricultural irrigation into the regional area of the aquifer. Excess recharge may cause soil liquefaction or wet basements of buildings. Groundwater flow behavior induced by recharge is therefore crucial in water resource management. The Boussinesq equation has been extendedly used to describe horizontal flow without the vertical component in unconfined aquifers (e.g., Ireson and Butler, 2013; van der Spek et al., 2013; Yeh and Chang, 2013; Chor and Dias, 2015; Hsieh et al., 2015; Liang and Zhang, 2015; Liang et al., 2015). The equation can be linearized by assuming uniform saturated aquifer thickness for developing its analytical solution. Marino (1967) presented quantitative criteria for the validity of the linearized Boussinesq equation. The criteria are introduced in the next section.

The rate of localized recharge can be a constant for a long term but should be dependent of time for a short term (Rai et al., 2006). An exponentially decaying function of time is usually used for recharge intensity decreasing from a certain rate to an ultimate one. An arbitrary time-depending recharge rate is commonly approximated as the combination of several linear segments of time to develop analytical solutions for water table rise subject to the recharge.

Analytical models accounting for water table rise due to recharge region of an infinite-length strip are reviewed. One-dimensional (1D) flow perpendicular to the strip is considered while the flow along the strip is assumed ignorable. These models deal with aquifers of infinite or finite extent with various types of outer boundary conditions. Hantush (1963) considered an aquifer of infinite extent without a lateral boundary. Rao and Sarma (1980) considered an aquifer of finite extent with two constant-head (also called Dirichlet) boundaries. Later, they developed a solution (Rao and Sarma, 1984) for a finite-extent aquifer between no-flow and constant-head boundaries. Latinopoulos (1986) deliberated on a finite-extent aquifer between two boundaries, one of which is under the Robin condition and the other is under either the

Dirichlet or no-flow condition. The recharge rate is treated as a periodical pulse consisting of constant rates for rainy seasons and zero for dry seasons. Bansal and Das (2010) studied an aquifer extending semi-infinitely from a Dirichlet boundary and overlying a sloping impervious base and indicated that the change in groundwater mound induced by strip-shaped recharge region increases with the base slope.

A variety of analytical models were presented to describe water table rise for two-dimensional (2D) flow induced by rectangle-shaped recharge into unconfined aquifers. The differences between these solutions are addressed below. Hantush (1967) considered an infinite-extent aquifer with localized recharge having a constant rate. Manglik et al. (1997) handled an arbitrary time-varying rate of recharge into a rectangular aquifer bounded by no-flow stratum. Manglik and Rai (1998) investigated flow behavior based on an irregularly time-varying rate of recharge into a rectangular aquifer with the lateral boundary under the Dirichlet condition. Bruggeman (1999) introduced an analytical solution for steady-state flow induced by localized recharge into a vertical strip aquifer between two Robin boundaries. Chang and Yeh (2007) considered one localized recharge and multiple extraction wells in an anisotropic aquifer overlying an impervious sloping bed. They indicated that the aquifer anisotropy and bottom slope notably influence water table distributions. Bansal and Teloglou (2013) explored the problem of a groundwater mound subject to multiple localized recharges and withdrawal wells in an unconfined aquifer overlying a semi-permeable base. They indicated that groundwater mound rises as decrease in the aquifer hydraulic conductivity.

Some articles discussed water table rise near circle-shaped recharge region and thus considered radial groundwater flow which is symmetric to the center of the region. Rai et al. (1998) presented an analytical model describing water table growth subject to an exponentially decaying rate of recharge in a circle-shaped unconfined aquifer with an outer Dirichlet boundary. Illas et al. (2008) considered the same model but a leaky aquifer. They indicated that leakage across the aquifer bottom significantly influences spatiotemporal water table distributions despite a small amount of the leakage. On the other hand, some researches considered radial flow having the vertical component near a circle-shaped recharge region of an infinite-extent unconfined aquifer. A first-order free surface equation as the top boundary condition of the aquifer is applied to describe water table rise. Zlotnik and Ledder (1992) developed analytical models for describing the distributions of hydraulic head and flow velocity due to constant-rate recharge. They found that models neglecting aquifer compressibility overestimate the magnitudes of the head and flow velocity. Ostendorf et al. (2007) derived an analytical model for head variation due to an exponentially decaying rate of recharge. Predictions of their solution agreed well with the field data obtained in the Plymouth-Carver Aquifer in southeastern Massachusetts given by Hansen and Lapham (1992).

Some studies developed a three-dimensional (3D) flow model based on the Laplace equation which neglects the aquifer compressibility effect. Dagan (1967) derived an analytical solution of the velocity potential caused by regional recharge into an unconfined aquifer of infinite thickness. Zlotnik and Ledder (1993) also developed an analytical solution of the same model but considered finite thickness for the unconfined aquifer. Predictions of their solution indicate that groundwater flow are horizontal in the area beyond 150% of the length or width of a rectangular recharge region.

It would be informative to summarize the above-mentioned models in Table 1. The solutions of the models are classified according to flow dimensions into 1D, 2D, 3D, and radial flows and further categorized according to aquifer domain, aquifer boundary conditions, recharge region, and recharge rate. The table shows that those solutions assume either no vertical flow or aquifer incompressibility. In addition, the Dirichlet and no-flow conditions considered by some of those solutions are not applicable to a boundary having a semi-permeable stratum, but the Robin condition is. The former two conditions are indeed special cases of the third one.

The objective of this paper is to develop a new mathematical model for depicting spatiotemporal hydraulic head distributions subject to localized recharge with an arbitrary time-varying recharge rate in a rectangular-shaped unconfined aquifer. The four boundaries are considered under the Robin condition which can reduce to the Dirichlet or no-flow condition. A governing equation describing 3D transient flow subject to the effect of aquifer compressibility is used. A first-order free surface equation with a source term representing recharge rate is chosen to describe the top boundary condition. The transient head solution of the model is derived by the methods of Laplace transform, double-integral transform, and Duhamel's theorem. The sensitivity analysis based on the present solution is performed to study the head response to the change in each of hydraulic parameters. On the basis of solution's predictions, the effect of the Robin boundaries on time-depending head distributions at observation points is investigated. A quantitative criterion under which the Robin condition reduces to the Dirichlet or no-flow one is provided. In addition, quantitative criteria for the validity of two assumptions of aquifer incompressibility and no vertical flow are provided and errors arising from the assumptions in the hydraulic head are also discussed. Temporal head distributions accounting for transient recharge rates are demonstrated as well.

## 2 Methodology

### 2.1 Mathematical model

A mathematical model is developed for describing spatiotemporal hydraulic head distributions induced by localized recharge in a rectangular unconfined aquifer as illustrated in Fig. 1a. The four boundaries of the aquifer are considered under the Robin condition. The aquifer has the widths of $l$ and $w$ in $x$- and $y$-directions, respectively. The recharge uniformly distributes over a rectangular region having widths $a$ and $b$ in $x$- and $y$-directions, respectively.

The lower left corner of the region is designated at ($x_1$, $y_1$). The shortest distances measured from the edge of the region to boundaries 1, 2, 3, and 4 are denoted as $d_1$, $d_2$, $d_3$, and $d_4$, respectively. The shortest distance between the edge of the region and an observation point at $(x, y)$ is defined as $d = \min(\sqrt{(x - x_e)^2 + (y - y_e)^2})$ where $(x_e, y_e)$ is a coordinate on the edge. The initial aquifer thickness is $B$ as shown in Fig. 1b.

The governing equation describing 3D transient head distributions in a homogeneous and anisotropic aquifer is expressed as

$$K_x \frac{\partial^2 h}{\partial x^2} + K_y \frac{\partial^2 h}{\partial y^2} + K_z \frac{\partial^2 h}{\partial z^2} = S_s \frac{\partial h}{\partial t} \tag{1}$$

where $t$ is time, $h(x, y, z, t)$ represents the hydraulic head, $K_x$, $K_y$, and $K_z$ are the hydraulic conductivities in $x$-, $y$-, and $z$-directions, respectively, and $S_s$ is the specific storage. The initial static water table is chosen as the reference datum where the elevation head is set to zero. The initial condition is therefore written as

$$h = 0 \quad \text{at} \quad t = 0 \tag{2}$$

The Robin conditions specified at the four sides of the aquifer are defined as

$$\frac{\partial h}{\partial x} - \frac{K_1}{K_x b_1} h = 0 \quad \text{at} \quad x = 0 \tag{3}$$

$$\frac{\partial h}{\partial x} + \frac{K_2}{K_x b_2} h = 0 \quad \text{at} \quad x = l \tag{4}$$

$$\frac{\partial h}{\partial y} - \frac{K_3}{K_y b_3} h = 0 \quad \text{at} \quad y = 0 \tag{5}$$

$$\frac{\partial h}{\partial y} + \frac{K_4}{K_y b_4} h = 0 \quad \text{at} \quad y = w \tag{6}$$

where subscripts 1, 2, 3, and 4 represent the boundaries at $x$ = 0, $x$ = $l$, $y$ = 0, and $y$ = $w$, respectively, and $K$ and $b$ are the hydraulic conductivity and width of the medium at the aquifer boundary, respectively. Note that each of Eqs. (3) – (6) reduces to the Dirichlet condition when $b$ (i.e., $b_1$, $b_2$, $b_3$, or $b_4$) is set to zero and the no-flow condition when $K$ (i.e., $K_1$, $K_2$, $K_3$, or $K_4$) is set to zero. The aquifer lies on an impermeable base denoted as

$$\partial h/\partial z = 0 \quad \text{at} \quad z = -B. \tag{7}$$

The first-order free surface equation describing the response of water table to recharge over the rectangular region can be written as (Zlotnik and Ledder, 1993)

$$K_z \frac{\partial h}{\partial z} + S_y \frac{\partial h}{\partial t} = I u_x u_y \quad \text{at} \quad z = 0 \tag{8}$$

$$u_x = u(x - x_1) - u(x - x_1 - a) \tag{8a}$$

$$u_y = u(y - y_1) - u(y - y_1 - b) \tag{8b}$$

where $S_y$ is the specific yield, $I$ is a recharge rate, and $u(\ )$ is the unit step function. Equation (8) involves the assumption of $I << K_z$ and the simplification from non-uniform saturated aquifer thickness below $z = h$ to uniform one below $z = 0$ (Dagan, 1967). Marino (1967) indicated that the simplification and assumption are valid when the water table rise is smaller than 50% of the initial water table height (i.e., $|h|/B < 0.5$) and the recharge rate is smaller than 20% of the hydraulic conductivity (i.e., $I/K_z < 0.2$). On the other hand, the effect of unsaturated flow above water table on model's predictions can be ignored when $\sigma B \geq 10^3$ where $\sigma$ is a parameter to define the relative hydraulic conductivity as $k_0 = \exp(-\sigma z)$ in the Richards' equation (Tartakovsky and Neuman, 2007). Tartakovsky and Neuman (2007) achieved agreement on aquifer drawdown evaluated by their analytical solution based on Eq. (1) for saturated flow and Richards' equation for unsaturated flow and by the Neuman (1974) solution based on Eqs. (1) and (8) with $I = 0$ when $\sigma B = 10^3$ (i.e., the case of $\kappa_D = 10^3$ in Fig. 2 in Tartakovsky and Neuman, 2007).

Dimensionless variables and parameters are defined as follows

$$\bar{h} = \frac{h}{B},\quad \bar{x} = \frac{x}{d},\quad \bar{y} = \frac{y}{d},\quad \bar{z} = \frac{z}{B},\quad \bar{l} = \frac{l}{d},\quad \bar{w} = \frac{w}{d},\quad \bar{x}_1 = \frac{x_1}{d},\quad \bar{y}_1 = \frac{y_1}{d},\quad \bar{a} = \frac{a}{d},\quad \bar{b} = \frac{b}{d},$$
$$\kappa_z = \frac{K_z d^2}{K_x B^2},\quad \bar{t} = \frac{K_x t}{S_s d^2},\quad \kappa_y = \frac{K_y}{K_x},\quad \kappa_1 = \frac{K_1 d}{K_x b_1},\quad \kappa_2 = \frac{K_2 d}{K_x b_2},\quad \kappa_3 = \frac{K_3 d}{K_y b_3},\quad \kappa_4 = \frac{K_4 d}{K_y b_4},\quad \xi =$$
$$\frac{I}{K_z},\quad \varepsilon = \frac{S_y}{S_s B},\quad \bar{d}_1 = \frac{d_1}{d},\quad \bar{d}_2 = \frac{d_2}{d},\quad \bar{d}_3 = \frac{d_3}{d},\quad \bar{d}_4 = \frac{d_4}{d} \tag{9}$$

where the overbar denotes a dimensionless symbol. Notice that the variables in the horizontal and vertical directions are divided by $d$ and $B$, respectively. According to Eq. (9), the mathematical model, Eqs. (1) – (8b), can then be expressed as

$$\frac{\partial^2 \bar{h}}{\partial \bar{x}^2} + \kappa_y \frac{\partial^2 \bar{h}}{\partial \bar{y}^2} + \kappa_z \frac{\partial^2 \bar{h}}{\partial \bar{z}^2} = \frac{\partial \bar{h}}{\partial \bar{t}} \tag{10}$$

$$\bar{h} = 0 \quad \text{at} \quad \bar{t} = 0 \tag{11}$$

$$\frac{\partial \bar{h}}{\partial \bar{x}} - \kappa_1 \bar{h} = 0 \quad \text{at} \quad \bar{x} = 0 \tag{12}$$

$$\frac{\partial \bar{h}}{\partial \bar{x}} + \kappa_2 \bar{h} = 0 \quad \text{at} \quad \bar{x} = \bar{l} \tag{13}$$

$$\frac{\partial \bar{h}}{\partial \bar{y}} - \kappa_3 \bar{h} = 0 \quad \text{at} \quad \bar{y} = 0 \tag{14}$$

$$\frac{\partial \bar{h}}{\partial \bar{y}} + \kappa_4 \bar{h} = 0 \quad \text{at} \quad \bar{y} = \bar{w} \tag{15}$$

$$\partial \bar{h}/\partial \bar{z} = 0 \quad \text{at} \quad \bar{z} = -1 \tag{16}$$

$$\frac{\partial \bar{h}}{\partial \bar{z}} + \frac{\varepsilon}{\kappa_z} \frac{\partial \bar{h}}{\partial \bar{t}} = \xi \bar{u}_x \bar{u}_y \quad \text{at} \quad \bar{z} = 0 \tag{17}$$

$$\bar{u}_x = u(\bar{x} - \bar{x}_1) - u(\bar{x} - \bar{x}_1 - \bar{a}) \tag{17a}$$

$$\bar{u}_y = u(\bar{y} - \bar{y}_1) - u\left(\bar{y} - \bar{y}_1 - \bar{b}\right). \tag{17b}$$

**2.2 Analytical solution**

The mathematical model, Eqs. (10) – (17b), can be solved by the methods of Laplace transform and double-integral transform. The former transform converts $\bar{h}(\bar{x}, \bar{y}, \bar{z}, \bar{t})$ into $\tilde{h}(\bar{x}, \bar{y}, \bar{z}, p)$, $\partial \bar{h}/\partial \bar{t}$ into $p\tilde{h} - \bar{h}|_{\bar{t}=0}$, and $\xi \bar{u}_x \bar{u}_y$ into $\xi \bar{u}_x \bar{u}_y / p$ where $p$ is the Laplace parameter and $\bar{h}|_{\bar{t}=0}$ equals zero in Eq. (11). After taking the transform, the model become a boundary value problem expressed as

$$\frac{\partial^2 \tilde{h}}{\partial \bar{x}^2} + \kappa_y \frac{\partial^2 \tilde{h}}{\partial \bar{y}^2} + \kappa_z \frac{\partial^2 \tilde{h}}{\partial \bar{z}^2} = p\tilde{h} \tag{18}$$

with boundary conditions $\partial \tilde{h}/\partial \bar{x} - \kappa_1 \tilde{h} = 0$ at $\bar{x} = 0$, $\partial \tilde{h}/\partial \bar{x} + \kappa_2 \tilde{h} = 0$ at $\bar{x} = \bar{l}$, $\tilde{h}/\partial \bar{y} - \kappa_3 \tilde{h} = 0$ at $\bar{y} = 0$, $\tilde{h}/\partial \bar{y} + \kappa_4 \tilde{h} = 0$ at $\bar{y} = \bar{w}$, $\partial \tilde{h}/\partial \bar{z} = 0$ at $\bar{z} = -1$, and $\partial \tilde{h}/$

$\partial \bar{z} + \varepsilon p \tilde{h} / \kappa_z = \xi \bar{u}_x \bar{u}_y / p$ at $\bar{z} = 0$. We then apply the properties of the double-integral transform to the problem. One can refer to the definition in Latinopoulos (1985, Table I, aquifer type 1). The transform turns $\tilde{h}(\bar{x}, \bar{y}, \bar{z}, p)$ into $\hat{h}(\alpha_m, \beta_n, \bar{z}, p)$, $\partial^2 \tilde{h} / \partial \bar{x}^2 + \kappa_y (\partial^2 \tilde{h} / \partial \bar{y}^2)$ into $-(\alpha_m^2 + \kappa_y \beta_n^2) \hat{h}$ where $(m, n) \in 1, 2, 3, \ldots \infty$, and eigenvalues $\alpha_m$ and $\beta_n$ are the positive roots of the following equations that

$$\tan(\bar{l}\alpha_m) = \frac{\alpha_m(\kappa_1 + \kappa_2)}{\alpha_m^2 - \kappa_1 \kappa_2} \tag{19}$$

and

$$\tan(\bar{w}\beta_n) = \frac{\beta_n(\kappa_3 + \kappa_4)}{\beta_n^2 - \kappa_3 \kappa_4}. \tag{20}$$

In addition, $\bar{u}_x \bar{u}_y$ defined in Eqs. (17a) and (17b) is transformed into $U_m U_n$ given by

$$U_m = \frac{\sqrt{2} V_m}{\sqrt{\kappa_1 + (\alpha_m^2 + \kappa_1^2)[\bar{l} + \kappa_2 / (\alpha_m^2 + \kappa_2^2)]}} \tag{21}$$

$$U_n = \frac{\sqrt{2} V_n}{\sqrt{\kappa_3 + (\beta_n^2 + \kappa_3^2)[\bar{w} + \kappa_4 / (\beta_n^2 + \kappa_4^2)]}} \tag{22}$$

with

$$V_m = \{\kappa_1[\cos(\alpha_m \bar{x}_1) - \cos(\alpha_m \chi)] - \alpha_m[\sin(\alpha_m \bar{x}_1) - \sin(\alpha_m \chi)]\} / \alpha_m \tag{23}$$

$$V_n = \{\kappa_3[\cos(\beta_n \bar{y}_1) - \cos(\beta_n \psi)] - \beta_n[\sin(\beta_n \bar{y}_1) - \sin(\beta_n \psi)]\} / \beta_n \tag{24}$$

where $\chi = \bar{x}_1 + \bar{a}$ and $\psi = \bar{y}_1 + \bar{b}$.

Equation (18) then reduces to an ordinary differential equation as

$$\kappa_z \frac{\partial^2 \hat{h}}{\partial \bar{z}^2} - (p + \alpha_m^2 + \kappa_y \beta_n^2) \hat{h} = 0 \tag{25}$$

Two boundary conditions are expressed, respectively, as

$$\partial \hat{h} / \partial \bar{z} = 0 \quad \text{at} \quad \bar{z} = -1 \tag{26}$$

and

$$\frac{\partial \hat{h}}{\partial \bar{z}} + \frac{\varepsilon p}{\kappa_z} \hat{h} = \frac{\xi}{p} U_m U_n \quad \text{at} \quad \bar{z} = 0. \tag{27}$$

Solving Eq. (25) with Eqs. (26) and (27) results in

$$\hat{h}(\alpha_m, \beta_n, \bar{z}, p) = \frac{\xi U_m U_n \cosh[(1+\bar{z})\lambda]}{p(p\varepsilon\kappa_z \cosh\lambda + \kappa_z \lambda \sinh\lambda)} \tag{28}$$

where

$$\lambda = \sqrt{(p + \alpha_m^2 + \kappa_y \beta_n^2)/\kappa_z}. \tag{29}$$

Inverting Eq. (28) to the space and time domains gives rise to the analytical solution that

$$\bar{h}(\bar{x}, \bar{y}, \bar{z}, \bar{t}) = \xi \sum_{m=1}^{\infty} \sum_{n=1}^{\infty} (\phi_{m,n} + \phi_{0,m,n} + \sum_{j=1}^{\infty} \phi_{j,m,n}) F_m F_n U_m U_n \tag{30}$$

with

$$\phi_{m,n} = \frac{\cosh[(1+\bar{z})\lambda_{m,n}]}{\kappa_z \lambda_{m,n} \sinh \lambda_{m,n}} \tag{30a}$$

$$\phi_{0,m,n} = -2\lambda_{0,m,n} \cosh[(1+\bar{z})\lambda_{0,m,n}] \exp(-\gamma_{0,m,n}\bar{t})/\eta_{0,m,n} \tag{30b}$$

$$\phi_{j,m,n} = -2\lambda_{j,m,n} \cos[(1+\bar{z})\lambda_{j,m,n}] \exp(-\gamma_{j,m,n}\bar{t})/\eta_{j,m,n} \tag{30c}$$

$$\eta_{0,m,n} = \gamma_{0,m,n}[(1+2\varepsilon\kappa_z)\lambda_{0,m,n} \cosh\lambda_{0,m,n} + \left(1 - \varepsilon\gamma_{0,m,n}\right) \sinh\lambda_{0,m,n}] \tag{30d}$$

$$\eta_{j,m,n} = \gamma_{j,m,n}[(1+2\varepsilon\kappa_z)\lambda_{j,m,n} \cos\lambda_{j,m,n} + \left(1 - \varepsilon\gamma_{j,m,n}\right) \sin\lambda_{j,m,n}] \tag{30e}$$

$$\lambda_{m,n} = \sqrt{f_{m,n}/\kappa_z};\ \gamma_{0,m,n} = f_{m,n} - \kappa_z \lambda_{0,m,n}^2;\ \gamma_{j,m,n} = f_{m,n} + \kappa_z \lambda_{j,m,n}^2 \tag{30f}$$

$$f_{m,n} = \alpha_m^2 + \kappa_y \beta_n^2 \tag{30g}$$

$$F_m = \frac{\sqrt{2}[\alpha_m \cos(\alpha_m \bar{x}) + \kappa_1 \sin(\alpha_m \bar{x})]}{\sqrt{\kappa_1 + (\alpha_m^2 + \kappa_1^2)[\bar{l} + \kappa_2/(\alpha_m^2 + \kappa_2^2)]}} \tag{30h}$$

$$F_n = \frac{\sqrt{2}[\beta_n \cos(\beta_n \bar{y}) + \kappa_3 \sin(\beta_n \bar{y})]}{\sqrt{\kappa_3 + (\beta_n^2 + \kappa_3^2)[\bar{w} + \kappa_4/(\beta_n^2 + \kappa_4^2)]}} \tag{30i}$$

where $j \in 1, 2, 3, \ldots \infty$ and eigenvalues $\lambda_{0,m,n}$ and $\lambda_{j,m,n}$ are determined, respectively, by the following equations that

$$\tan\lambda_{j,m,n} = -\varepsilon(f_{m,n} + \kappa_z \lambda_{j,m,n}^2)/\lambda_{j,m,n} \tag{31}$$

and

$$\frac{-\varepsilon\kappa_z \lambda_{0,m,n}^2 + \lambda_{0,m,n} + \varepsilon f_{m,n}}{\varepsilon\kappa_z \lambda_{0,m,n}^2 + \lambda_{0,m,n} - \varepsilon f_{m,n}} = \exp(2\lambda_{0,m,n}). \tag{32}$$

Notice that Eqs. (19), (20), and (31) have infinite positive roots owing to the trigonometric function tan( ) while Eq. (32) has only one positive root. The method to find $\alpha_m$, $\beta_n$, $\lambda_{j,m,n}$ and $\lambda_{0,m,n}$ is introduced in Sect. 2.3. One can refer to Appendix A for the derivation of Eq. (30). The first term on the right-hand side (RHS) of Eq. (30) is a double series expanded by $\alpha_m$ and $\beta_n$. The series converges within a few terms because the power of $\alpha_m$ (or $\beta_n$) in the denominator of $\phi_{m,n}$ in Eq. (30a) is two more than that in the nominator. The second term on the RHS of Eq. (30) is a double series expanded by $\alpha_m$ and $\beta_n$, and the third term is a triple series expanded by $\alpha_m$, $\beta_n$, and $\lambda_{j,m,n}$. They converge very fast due to exponential functions in Eqs. (30b) and (30c). Consider $(m, n) \in (1, 2, \ldots, N = 30)$ and $j \in (1, 2, \ldots, N_j = 15)$ for the default values of dimensionless parameters and variables in Table 2 for calculation. The number of terms in one or the other double series is $30 \times 30 = 900$ and in the triple series is $30 \times 30 \times 15 = 13500$. The total number is therefore $900 \times 2 + 13500 = 15300$. We apply Mathematica FindRoot routine to obtain the values of $\alpha_m$, $\beta_n$, and $\lambda_{j,m,n}$ and Sum routine to compute the double and triple series. It takes about 8 seconds to finish calculation for $\bar{t} = 10^5$ by a personal computer with Intel Core i5-4590 3.30 GHz processor and 8 GB RAM. In addition, the series is considered to converge when the absolute value of the last term in the double series of $\phi_{m,n}$ is smaller than $10^{-20}$ (i.e., $10^{-50} < 10^{-20}$ in this case). That value in the other double or triple series may be even smaller than $10^{-50}$ due to exponential decay.

The use of finite aquifer domain has two merits. One is that the solution of depth-average head, defined as $\int_{-1}^{0} \bar{h}(\bar{x}, \bar{y}, \bar{z}, \bar{t})\, d\bar{z}$, can be analytically integrated. The integration variable $\bar{z}$ appears only in the functions of $\cosh[(1+\bar{z})\lambda_{m,n}]$ in Eq. (30a), $\cosh[(1+\bar{z})\lambda_{0,m,n}]$ in Eq. (30b) and $\cos[(1+\bar{z})\lambda_{j,m,n}]$ in Eq. (30c). The solution of depth-average head therefore equals Eq. (30) where these three functions are replaced by $\sinh\lambda_{m,n}/\lambda_{m,n}$, $\sinh\lambda_{0,m,n}/\lambda_{0,m,n}$, and $\sin\lambda_{j,m,n}/\lambda_{j,m,n}$, respectively. The other is that the present solution is applicable to head predictions in aquifers of infinite extent before the dimensionless time to have lateral aquifer boundary effect on the predictions. Wang and Yeh (2008) reported a time criterion defined as $\bar{t}_{cr} = 0.03(1+\varepsilon)\bar{R}^2$ where $\bar{R} = R/d$ denotes a shortest dimensionless distance from the lateral boundary to the edge of the recharge region. This criterion is, in effect, a boundary-effect time when the hydraulic head is affected by the aquifer boundary. Existing solutions based on aquifers of infinite extent can therefore be considered as special cases of the present solution before the boundary-effect time.

### 2.3 Calculation of eigenvalues

The eigenvalues $\alpha_m$, $\beta_n$, $\lambda_{j,m,n}$, and $\lambda_{0,m,n}$ can be determined by Newton's method with initial guess values (IGVs) set to be the vertical asymptotes of the functions on the left-hand side (LHS) of Eqs. (19), (20), (31), and (32), respectively. Hence, IGVs for $\alpha_m$ are $\alpha' + \delta$ if $\alpha' < (\kappa_1\kappa_2)^{1/2}$ and $\alpha' - \delta$ if $\alpha' > (\kappa_1\kappa_2)^{1/2}$ where $\alpha' = (2m-1)\pi/(2\bar{l})$ and $\delta$ is a small value of $10^{-8}$ to avoid being right at the vertical asymptotes. Similarly, IGVs for $\beta_n$ are $\beta' + \delta$ if $\beta' < (\kappa_3\kappa_4)^{1/2}$ and $\beta' - \delta$ if $\beta' > (\kappa_3\kappa_4)^{1/2}$ where $\beta' = (2n-1)\pi/(2\bar{w})$. In addition, IGVs for $\lambda_{j,m,n}$ are $(2j-1)\pi/2 + \delta$, and IGV for $\lambda_{0,m,n}$ is $\delta + \left[\left(1 + 4\kappa_z f_{m,n}\varepsilon^2\right)^{1/2} - 1\right]/(2\varepsilon\kappa_z)$ obtained by setting the denominator of the LHS function of Eq. (32) to be zero and solving the resultant equation.

### 2.4 Solution for time-varying recharge rate

The present solution, Eq. (30), is applicable to arbitrary time-depending recharge rates on the basis of Duhamel's theorem expressed as (e.g., Bear, 1979, p. 158)

$$\bar{h}_{It} = \bar{h}_{I0} + \int_0^{\bar{t}} \frac{\partial \xi_t(\tau)}{\partial \tau} \bar{h}(\bar{t} - \tau)/\xi \, d\tau \qquad (33)$$

where $\bar{h}_{It}$ signifies a dimensionless head solution for a time-depending recharge rate $\xi_t(\tau)$ with $\bar{t}$ replaced by $\tau$, $\bar{h}_{I0}$ is Eq. (30) in which $\xi$ is replaced by $\xi_t(0)$, and $\bar{h}(\bar{t} - \tau)$ is also

Eq. (30) with $\bar{t}$ replaced by $\bar{t}-\tau$. If Eq. (33) is not integrable, it can be discretized as (Singh, 2005)

$$\bar{h}_N = \sum_{i=1}^{N} \frac{\Delta\xi_i}{\Delta\bar{t}} \eta(N-i+1) \tag{34}$$

with

$$\Delta\xi_i = \xi_i - \xi_{i-1} \tag{34a}$$

$$\eta(M) = \int_0^{\bar{t}} \bar{h}(M\Delta\bar{t}-\tau)d\tau \tag{34b}$$

where $\bar{h}_N$ represents a numerical result of dimensionless head $\bar{h}$ at $\bar{t} = \Delta\bar{t} \times N$, $\Delta\bar{t}$ is a dimensionless time step, $\xi_i$ and $\xi_{i-1}$ are dimensionless recharge rates at $\bar{t} = \Delta\bar{t} \times i$ and $\bar{t} = \Delta\bar{t} \times (i-1)$, respectively, and $\eta(M)$, called ramp kernel, depends on Eq. (30) in which $\bar{t}$ is replaced by $M\Delta\bar{t}-\tau$. The integration result of Eq. (34b) can be denoted as Eq. (30) where $\phi_{m,n}$ is replaced by $\phi_{m,n}\bar{t}$ and two exponential terms in Eqs. (30b) and (30c) are replaced, respectively, by $\exp(-M\gamma_{0,m,n}\Delta\bar{t})\left[-1+\exp(\gamma_{0,m,n}\Delta\bar{t})\right]/\gamma_{0,m,n}$ and $\exp(-M\gamma_{j,m,n}\Delta\bar{t})\left[-1+\exp(\gamma_{j,m,n}\Delta\bar{t})\right]/\gamma_{j,m,n}$.

### 2.5 Sensitivity analysis

The sensitivity analysis is administered to assess the change in the hydraulic head in response to the change in each of the hydraulic parameters. The normalized sensitivity coefficient of the hydraulic head to a specific parameter can be expressed as

$$S_{c,t} = \frac{\partial h/B}{\partial P_c/P_c} = \frac{\partial \bar{h}}{\partial P_c/P_c} \tag{35}$$

where $P_c$ is the $c$-th parameter in the present solution, $S_{c,t}$ is the coefficient at a time to the $c$-th parameter, and $\bar{h}$ is the present solution, Eq. (30). The derivative in Eq. (35) can be approximated as

$$S_{c,t} = \frac{\bar{h}(P_c+\Delta P_c)-\bar{h}(P_c)}{\Delta P_c/P_c} \tag{36}$$

where $\Delta P_c$ is an increment chosen as $10^{-3} P_c$ (Yeh et al., 2008).

## 3 Results and discussion

Previous articles have discussed groundwater mounds in response to localized recharge into aquifers with various hydraulic parameters (e.g., Dagan, 1967; Rao and Sarma, 1980; Latinopoulos, 1986; Manglik et al., 1997; Manglik and Rai, 1998; Rai et al., 1998; Chang and Yeh, 2007; Illas et al., 2008; Bansal and Das, 2010; Bansal and Teloglou, 2013). Flow velocity fields below groundwater mounds have also been analyzed (Zlotnik and Ledder, 1992; Zlotnik and Ledder, 1993). This section therefore focuses on the transient behavior of hydraulic head at an observation point with the aid of the present solution. The default values of the parameters and variables for calculation are noted in Table 2. In Sect. 3.1, transient head distributions subject to Dirichlet, no-flow and Robin boundary conditions are compared. In Sect. 3.2, the effect of vertical flow on the head distribution is investigated. In Sect. 3.3, errors arising from assuming aquifer incompressibility (i.e., $S_s$ = 0) to develop analytical solutions are discussed. In Sect. 3.4, the response of the hydraulic head to transient recharge rates based on Eq. (33) is demonstrated. In Sect. 3.5, the sensitivity analysis defined by Eq. (36) is performed.

### 3.1 Effect of lateral boundary

The Robin condition can become the Dirichlet or no-flow one, depending on the magnitudes of $\kappa_1 \bar{d}_1$ for Eq. (12), $\kappa_2 \bar{d}_2$ for Eq. (13), $\kappa_3 \bar{d}_3$ for Eq. (14), and $\kappa_4 \bar{d}_4$ for Eq. (15). We consider a symmetrical aquifer system with $\bar{l} = \bar{w} = 22$, $\bar{d}_1 = \bar{d}_2 = \bar{d}_3 = \bar{d}_4 = 10$ and $\kappa_1 = \kappa_2 = \kappa_3 = \kappa_4$ ~~as illustrated in Fig. 2~~. The magnitudes of $\kappa_1 \bar{d}_1$, $\kappa_2 \bar{d}_2$, $\kappa_3 \bar{d}_3$ and $\kappa_4 \bar{d}_4$ are the same and defined as $\kappa$. The curves of $\bar{h}$ versus $\bar{t}$ plotted by the present solution, Eq. (30), for $\kappa = 10^{-3}, 10^{-2}, 10^{-1}$, 1, 10, 100, and 200 are shown in Fig. 2. The curves $\bar{h}$ versus $\bar{t}$ are plotted from Manglik et al. (1997) solution with the no-flow condition (i.e., $\kappa$

= 0), Manglik and Rai (1998) solution with the Dirichlet condition (i.e., $\kappa \to \infty$), and the present solution with the Robin condition. Before $\bar{t}$ = $10^4$, these curves give the same magnitude of $\bar{h}$ at a fixed dimensionless time $\bar{t}$ since the lateral aquifer boundary has been beyond the place where groundwater is affected by localized recharge. After $\bar{t}$ = $10^4$, the curves for the cases of $\kappa$ = $10^{-2}$, $10^{-1}$, 1, 10, and 100 deviate from each other gradually as time increases. A larger magnitude of $\kappa$ between $\kappa$ = $10^{-2}$ and $\kappa$ = 100 causes a smaller $\bar{h}$ at a fixed $\bar{t}$. On the other hand, the present solution for the cases of $\kappa$ = $10^{-3}$ and $10^{-2}$ agrees well with Manglik et al. (1997) solution based on $\kappa$ = 0 and that for the cases of $\kappa$ = 100 and 200 predicts the same result as Manglik and Rai (1998) solution based on $\kappa \to \infty$. We may reasonably conclude that the Robin condition reduces to the no-flow one when $\kappa \leq 10^{-2}$ and the Dirichlet one when $\kappa \geq 100$.

### 3.2 Effect of vertical flow

Dimensionless parameter $\kappa_z$ (i.e., $K_z d^2/(K_x B^2)$) dominates the effect of vertical flow on transient head distributions at an observation point. Consider $\kappa_1 \bar{d}_1 = \kappa_2 \bar{d}_2 = \kappa_3 \bar{d}_3 = \kappa_4 \bar{d}_4 = 100$ for lateral aquifer boundaries under the Dirichlet condition as discussed in Sect. 3.1. The temporal distributions of $\bar{h}$ predicted by the present solution, Eq. (30), with $\kappa_z$ = 0.01, 0.1, 1, and 10 are demonstrated in Fig. 3. The temporal distribution of $\bar{h}$ predicted by Manglik and Rai (1998) solution based on 2D flow without the vertical component is taken in order to address the effect of vertical flow. The figure reveals that $\bar{h}$ increases with $\kappa_z$ when $\kappa_z \leq 1$. The difference in $\bar{h}$ predicted by both solutions indicates the vertical flow effect. The Manglik and Rai (1998) solution obviously overestimates the head. The vertical flow prevails, and its effect should be taken into account when $\kappa_z < 1$, indicating a thick aquifer, a small ratio of $K_z/K_x$, and/or an observation point near a recharge region. On the other hand, the present solution for the cases of $\kappa_z$ = 1 and 10 agrees well with Manglik and Rai (1998) solution, indicating that the vertical flow effect is ignorable when $\kappa_z \geq 1$. We can recognize from the agreement that existing solutions neglecting the vertical flow effect give good predictions when $\kappa_z \geq 1$.

### 3.3 Effect of specific storage

Some of existing models use the Laplace equation as a governing equation with assuming $S_s$ = 0 (e.g., Singh, 1976; Schmitz and Edenhofer, 1988; Zlotnik and Ledder, 1993). The assumption is valid when $\varepsilon$ (i.e., $S_y/(S_sB)$) is larger than a certain value. This section quantifies the value. The Zlotnik and Ledder (1993) model based on 3D Laplace equation, Eq. (1) with $S_s$ = 0, is taken for comparison with the present model using Eq. (1) with $S_s \neq 0$. The dimensionless variables of *s*, *x*, *y*, *z*, *t*, *X*, and *Y* in their model are replaced by $\bar{h}/\xi$, $(\kappa_z)^{1/2}\bar{x}$, $(\kappa_z)^{1/2}\bar{y}$, $\bar{z}$, $\kappa_z\bar{t}/\varepsilon$, $(\kappa_z)^{1/2}\bar{a}$, and $(\kappa_z)^{1/2}\bar{b}$, respectively, for ease of comparisons. Consider the cases of $\kappa_z = 10^{-2}$ for an observation point located at a 3D flow area and $\kappa_z = 10$ for the point located at a 2D flow area as discussed in Sect. 3.2. The assumption can be assessed through the comparison in the dimensionless heads predicted by both solutions for $\varepsilon$ = 1, 10, $10^2$, and $10^3$ as shown in Fig. 4a for $\kappa_z = 10^{-2}$ and Fig. 4b for $\kappa_z = 10$. The present solution predicts a steady-state $\bar{h}$ of 0.054 in Fig. 4a and 0.074 in Fig. 4b after certain times due to lateral Dirichlet boundaries (i.e., $\kappa_1\bar{d}_1 = \kappa_2\bar{d}_2 = \kappa_3\bar{d}_3 = \kappa_4\bar{d}_4 = 100$) as discussed in Sect. 3.1. In contrast, their solution predicts $\bar{h}$ which increases with $\bar{t}$ due to the absence of lateral boundaries. When $\varepsilon$ = 1 and 10, both solutions give different values of $\bar{h}$ for both cases of $\kappa_z = 10^{-2}$ and $\kappa_z = 10$ before $\bar{t}$ = 100, indicating that the assumption of $S_s$ = 0 causes inaccurate $\bar{h}$. When $\varepsilon$ = $10^2$ and $10^3$, both solutions predict very close results of $\bar{h}$ for both cases before the time of approaching steady-state $\bar{h}$. These results lead to the conclusion that the assumption of $S_s$ = 0 is valid when $\varepsilon \geq 100$ for 3D and 2D flow cases.

### 3.4 Transient recharge rate

Most articles (e.g., Rai et al., 1998; Chang and Yeh, 2007; Illas et al., 2008; Bansal and Teloglou, 2013) define a transient recharge rate as $I_t(t) = I_1 + I_0 \exp(-rt)$ (i.e., $\xi_t(\bar{t}) = \xi_1 + \xi_0 \exp(-\gamma\bar{t})$ for a dimensionless rate) where $\xi_t = I_t/K_z$, $\xi_1 = I_1/K_z$, $\xi_0 = I_0/K_z$, $\gamma = rS_s d^2/K_x$, and $r$ is a decay constant. The rate exponentially declines from an initial value of $I_1 + I_0$ to an ultimate one of $I_1$. The present solution, Eq. (30), can be applied for the response of the head to the transient rate based on Eq. (33). Substituting $\partial\xi_t(\tau)/\partial\tau = -\gamma\xi_0 \exp(-\gamma\tau)$ into Eq. (33) and integrating the result for $\tau$ from $\tau = 0$ to $\tau = \bar{t}$ yields $\bar{h}_{I0}$ plus Eq. (30) where $\xi$ in Eq. (30), $\phi_{m,n}$ in Eq. (30a), $\exp(-\gamma_{0,m,n}\bar{t})$ in (30b), and $\exp(-\gamma_{j,m,n}\bar{t})$ in (30c) are replaced by $\xi_0$, $\phi_{m,n}[\exp(-\gamma\bar{t}) - 1]$, $\gamma\left[\exp(-\gamma\bar{t}) - \exp\left(\gamma_{0,m,n}\bar{t}\right)\right]/(\gamma_{0,m,n} + \gamma)$, and $\gamma\left[\exp(-\gamma\bar{t}) - \exp\left(\gamma_{j,m,n}\bar{t}\right)\right]/(\gamma_{j,m,n} + \gamma)$, respectively. Similarly, Zlotnik and Ledder (1993) solution can also be used to obtain the head subject to the transient rate by substituting it into Eq. (33) and then integrating the result using numerical approaches. Now, we consider Ramana et al. (1995) solution depicting 2D flow induced by the transient rate in rectangular aquifers with the lateral boundaries under the Dirichlet condition. Figure 5 shows the temporal distributions of $\bar{h}$ for the transient rate predicted by these three solutions when $\kappa_z = 1$, $\kappa = 100$, and $\varepsilon = 100$. The present solution agrees well with Ramana et al. (1995) solution. We can recognize from the agreement that, even for transient rates, the Robin condition reduces to the Dirichlet one when $\kappa \geq 100$ (i.e., $\kappa_1\bar{d}_1 = \kappa_2\bar{d}_2 = \kappa_3\bar{d}_3 = \kappa_4\bar{d}_4 = 100$) as discussed in Sect. 3.1 and the vertical flow effect is ignorable when $\kappa_z \geq 1$ as discussed in Sect. 3.2. Moreover, agreement on $\bar{h}$ estimated by the present solution and Zlotnik and Ledder (1993) solution before $\bar{t} = 3 \times 10^3$ will make clear that, even for transient rates, assuming aquifer incompressibility (i.e., $S_s = 0$) is valid when $\varepsilon \geq 100$ as discussed in Sect. 3.3.

### 3.5 Sensitivity analysis

Consider point A of (555 m, 500 m, −10 m) at a 3D flow region (i.e., $\kappa_z < 1$) and point B of (800 m, 500 m, −10 m) at a 2D flow region (i.e., $\kappa_z \geq 1$) as discussed in Sect. 3.2. Localized recharge distributes over the square area of 450 m ≤ $x$ ≤ 550 m and 450 m ≤ $y$ ≤ 550 m. The distance $d$ herein is set to 5 m for point A and 250 m for point B. The aquifer system is of isotropy with $K_x = K_y$ and symmetry with $K_1 = K_2 = K_3 = K_4$ for conciseness. The sensitivity analysis is performed by Eq. (36) to investigate the responses of the hydraulic heads at these two points to the change in each of $a$, $b$, $S_s$, $S_y$, $K_x$ (or $K_y$), $K_z$, and $K_1$ (or $K_2$, $K_3$, and $K_4$). The curves of the normalized sensitivity coefficient $S_{c,t}$ versus $t$ for these seven parameters are shown in Fig. 6a for point A and Fig. 6b for point B. The figure shows that the hydraulic heads at both points are more sensitive to the changes in $a$, $b$, $K_x$, and $S_y$ than those in the others. This may indicate that a flow model should include at least these four parameters. The figure also shows that the heads at points A and B are insensitive to the change in $K_1$ because of $\kappa_1 \bar{d}_1$ = 4500 > 100 as discussed in Sect. 3.1. In addition, $S_{c,t}$ to $K_z$ for point A is nonzero after $t$ = 0.4 day due to $\kappa_z = 6.25 \times 10^{-3} < 1$ as discussed in Sect. 3.2. In contrast, $S_{c,t}$ to $K_z$ for point B is very close to zero over the entire period because of $\kappa_z$ = 15.625 > 1. Moreover, the heads at points A and B are insensitive to the change in $S_s$ due to $\varepsilon$ = 500 > 100 as discussed in Sect. 3.3.

## 4 Conclusions

A mathematical model is developed to depict spatiotemporal head distributions induced by localized recharge with an arbitrary time-varying rate in a rectangular unconfined aquifer bounded by Robin boundaries with different hydraulic parameters. A governing equation for 3D flow is considered. A first-order free surface equation with a source term representing the recharge is employed for describing the water table movement. The analytical head solution of the model is obtained by applying the Laplace transform, the double-integral transform, and

Duhamel's theorem. The use of rectangular aquifer domain leads to two merits. One is that the integration for the solution of the depth-average head can be analytically done. The other is that existing solutions based on aquifers of infinite extent are special cases of the present solution when the recharge time is less than the boundary-effect time. The present solution is applicable under the conditions of aquifer homogeneity, $|h|/B < 0.5$, $I/K_z < 0.2$, and $\sigma B \geq 10^3$ due to Eq. (8) neglecting the effect of unsaturated flow above water table (Marino, 1967; Tartakovsky and Neuman, 2007). The sensitivity analysis is performed to explore the response of the head to the change in each of hydraulic parameters. With the aid of the present solution, the following conclusions can be drawn:

1. In respect of affecting $\bar{h}$ at observation points, the Robin condition specified at $\bar{x} = 0$ reduces to the Dirichlet one when $\kappa_1 \bar{d}_1 \geq 100$ (i.e., $K_1 d_1/(K_x b_1) \geq 100$) and no-flow one when $\kappa_1 \bar{d}_1 \leq 10^{-2}$. The quantitative criteria for $\kappa_1 \bar{d}_1$ are applicable to $\kappa_2 \bar{d}_2$, $\kappa_3 \bar{d}_3$, and $\kappa_4 \bar{d}_4$ for the Robin conditions specified at $\bar{x} = \bar{l}$, $\bar{y} = 0$, and $\bar{y} = \bar{w}$, respectively.
2. The vertical flow causes significant decrease in the hydraulic head at an observation point when $\kappa_z < 1$ (i.e., $K_z d^2/(K_x B^2) < 1$). When $\kappa_z \geq 1$, the effect of vertical flow on the head is ignorable, and conventional models considering 2D flow without the vertical component can therefore predict accurate results.
3. The 3D Laplace equation based on the assumption of $S_s = 0$ can be regarded as a flow governing equation when $\varepsilon \geq 100$ (i.e., $S_y/(S_s B) \geq 100$) for the whole aquifer domain. Otherwise, head predictions based on the Laplace equation are overestimated.
4. The abovementioned conclusions are also applicable to problems of groundwater flow subject to recharge with arbitrary time-varying rates.

## Appendix A: Derivation of Eq. (30)

Let us start with function $G(p)$ from Eq. (28) that

$$G(p) = \frac{\cosh[(1+\bar{z})\lambda]}{p(p\varepsilon\kappa_z \cosh\lambda + \kappa_z \lambda \sinh\lambda)} \tag{A1}$$

with

$$\lambda = \sqrt{(p + f_{m,n})/\kappa_z} \tag{A2}$$

where $f_{m,n} = \alpha_m^2 + \kappa_y \beta_n^2$. Equation (A1) is a single-value function to $p$ in the complex plane because satisfying $G(p^+) = G(p^-)$ where $p^+$ and $p^-$ are the polar coordinates defined, respectively, as

$$p^+ = r_a \exp(i\theta) - f_{m,n} \tag{A3}$$

and

$$p^- = r_a \exp[i(\theta - 2\pi)] - f_{m,n} \tag{A4}$$

where $r_a$ represents a radial distance from the origin at $p = -f_{m,n}$, $i = \sqrt{-1}$ is the imaginary unit, and $\theta$ is an argument between 0 and $2\pi$. Substitute $p = p^+$ in Eq. (A3) into Eq. (A2), and we have

$$\lambda = \sqrt{r_a/\kappa_z} \exp(i\theta/2) = \sqrt{r_a/\kappa_z}\,[\cos(\theta/2) + i \sin(\theta/2)] \tag{A5}$$

Similarly, we can have

$$\lambda = \sqrt{r_a/\kappa_z} \exp[i(\theta - 2\pi)/2] = -\sqrt{r_a/\kappa_z}\,[\cos(\theta/2) + i \sin(\theta/2)] \tag{A6}$$

after $p$ in Eq. (A2) is replaced by $p^-$ in Eq. (A4). Substitution of Eqs. (A3) and (A5) into Eq. (A1) yields the same result as that obtained by substituting Eqs. (A4) and (A6) into Eq. (A1), indicating that Eq. (A1) is a single-value function without branch cut and its inverse Laplace transform equals the sum of residues for poles in the complex plane.

The residue for a simple pole can be formulated as

$$Res = \lim_{p \to \varphi} G(p) \exp(p\bar{t})\,(p - \varphi) \tag{A7}$$

where $\varphi$ is the location of the pole of $G(p)$ in Eq. (A1). The function $G(p)$ has infinite simple poles at the negative part of the real axis in the complex plane. The locations of these poles are the roots of equation that

$$p(p\varepsilon\kappa_z \cosh\lambda + \kappa_z\lambda\sinh\lambda) = 0 \tag{A8}$$

which is obtained by letting the denominator in Eq. (A1) to be zero. Obviously, one pole is at $p$ = 0, and its residue based on Eqs. (A1) and (A7) with $\lambda_{m,n} = \sqrt{f_{m,n}/\kappa_z}$ can be expressed as

$$\phi_{m,n} = \cosh\left[(1+\bar{z})\lambda_{m,n}\right]/(\kappa_z\lambda_{m,n}\sinh\lambda_{m,n}) \tag{A9}$$

The locations of other poles of $G(p)$ are the roots of the equation that

$$p\varepsilon\kappa_z \cosh\lambda + \kappa_z\lambda\sinh\lambda = 0 \tag{A10}$$

which is the expression in the parentheses in Eq. (A8). One pole is between $p = 0$ and $p = -f_{m,n}$. Let $\lambda = \lambda_{0,m,n}$, and Eq. (A2) becomes $p = -f_{m,n} + \kappa_z\lambda_{0,m,n}^2$. Substituting $\lambda = \lambda_{0,m,n}$, $p = -f_{m,n} + \kappa_z\lambda_{0,m,n}^2$, $\cosh\lambda_{0,m,n} = [\exp\lambda_{0,m,n} + \exp(-\lambda_{0,m,n})]/2$ and $\sinh\lambda_{0,m,n} = \left[\exp\lambda_{0,m,n} - \exp(-\lambda_{0,m,n})\right]/2$ into Eq. (A9) and rearranging the result lead to Eq. (32). The pole is at $p = -f_{m,n} + \kappa_z\lambda_{0,m,n}^2$ with a numerical value of $\lambda_{0,m,n}$. With Eq. (A1), Eq. (A7) equals

$$Res = \lim_{p\to\varphi} \frac{\cosh[(1+\bar{z})\lambda]}{p(p\varepsilon\kappa_z\cosh\lambda + \kappa_z\lambda\sinh\lambda)} \exp(p\bar{t})\,(p-\varphi) \tag{A11}$$

Apply L'Hospital's Rule to Eq. (A11), and then we have

$$Res = \lim_{p\to\varphi} \frac{-2\lambda\cosh[(1+\bar{z})\lambda]}{p[(1+2\varepsilon\kappa_z)\lambda\cosh\lambda + (1-\varepsilon p)\sinh\lambda]} \exp(p\bar{t}) \tag{A12}$$

The residue for the pole at $p = -f_{m,n} + \kappa_z\lambda_{0,m,n}^2$ can be defined as

$$\phi_{0,m,n} = \frac{-2\lambda_{0,m,n}\cosh[(1+\bar{z})\lambda_{0,m,n}]\exp(-\gamma_{0,m,n}\bar{t})}{\gamma_{0,m,n}[(1+2\varepsilon\kappa_z)\lambda_{0,m,n}\cosh\lambda_{0,m,n} + (1-\varepsilon\gamma_{0,m,n})\sinh\lambda_{0,m,n}]} \tag{A13}$$

which is obtained by Eq. (A12) with $\lambda = \lambda_{0,m,n}$ and $p = -f_{m,n} + \kappa_z\lambda_{0,m,n}^2 = \gamma_{0,m,n}$. On the other hand, infinite poles behind $p = -f_{m,n}$ are at $p = \gamma_{j,m,n}$ where $j \in 1, 2, 3, \ldots \infty$. Let $\lambda = \sqrt{-1}\lambda_{j,m,n}$, and Eq. (A2) yields $p = -f_{m,n} - \kappa_z\lambda_{j,m,n}^2$. Substituting $\lambda = \sqrt{-1}\lambda_{j,m,n}$, $p = -f_{m,n} - \kappa_z\lambda_{j,m,n}^2$, $\cosh\left(\sqrt{-1}\lambda_{j,m,n}\right) = \cos\lambda_{j,m,n}$, and $\sinh\left(\sqrt{-1}\lambda_{j,m,n}\right) = \sqrt{-1}\,\sin\lambda_{j,m,n}$ into Eq. (A9) and rearranging the result gives rise to Eq. (31). These poles are at $p = -f_{m,n} -$

$\kappa_z \lambda_{j,m,n}^2$ with numerical values of $\lambda_{j,m,n}$. On the basis of Eq. (A12) with $\lambda = \sqrt{-1}\lambda_{j,m,n}$ and $p = -f_{m,n} - \kappa_z \lambda_{j,m,n}^2 = \gamma_{j,m,n}$, the residues for these poles at $p = -f_{m,n} - \kappa_z \lambda_{j,m,n}^2$ can be expressed as

$$\phi_{j,m,n} = \frac{-2\lambda_{j,m,n}\cos[(1+\bar{z})\lambda_{j,m,n}]\exp(-\gamma_{j,m,n}\bar{t})}{\gamma_{j,m,n}[(1+2\varepsilon\kappa_z)\lambda_{j,m,n}\cos\lambda_{j,m,n} + (1-\varepsilon\gamma_{j,m,n})\sin\lambda_{j,m,n}]} \tag{A14}$$

As a result, the inverse Laplace transform for Eq. (A1) is the sum of Eqs. (A9) and (A13) and a simple series expended in the RHS function in Eq. (A14) (i.e., $\phi_{m,n} + \phi_{0,m,n} + \sum_{j=1}^{\infty}\phi_{j,m,n}$). Finally, Eq. (30) can be derived after taking the inverse double-integral transform for the result using the formula that (Latinopoulos, 1985, Eq. (14))

$$\bar{h}(\bar{x},\bar{y},\bar{z},\bar{t}) = \xi \sum_{m=1}^{\infty}\sum_{n=1}^{\infty}(\phi_{m,n} + \phi_{0,m,n} + \sum_{j=1}^{\infty}\phi_{j,m,n}) F_m F_n U_m U_n \tag{A15}$$

where $\xi$ and $U_m U_n$ result from $\xi U_m U_n$ in Eq. (28).


## Acknowledgements

This study has been partly supported by the Taiwan Ministry of Science and Technology under the grants MOST 103-2221-E-009-156 and MOST 104-2221-E-009-148-MY2. The computer software used to generate the results in Figures 2–6 is available upon request. The authors would like to thank the editor, Prof. Alberto Guadagnini, and two reviewers for their valuable and constructive comments.


## References


Bansal, R. K., and Das, S. K.: Analytical Study of Water Table Fluctuation in Unconfined Aquifers due to Varying Bed Slopes and Spatial Location of the Recharge Basin, J Hydrol Eng, 15, 909-917, 2010.

Bansal, R. K., and Teloglou, I. S.: An Analytical Study of Groundwater Fluctuations in Unconfined Leaky Aquifers Induced by Multiple Localized Recharge and Withdrawal, Global Nest J, 15, 394-407, 2013.

Bear, J.: Hydraulics of Groundwater, McGraw-Hill, New York, 158, 1979.

Bruggeman, G. A.: Analytical Solutions of Geohydrological Problems, Elsevier, Netherlands, 326, 1999.

Chang, Y. C., and Yeh, H. D.: Analytical solution for groundwater flow in an anisotropic sloping aquifer with arbitrarily located multiwells, J Hydrol, 347, 143-152, 2007.

Chor, T. L., and Dias, N. L.: Technical Note: A simple generalization of the Brutsaert and Nieber analysis, Hydrol Earth Syst Sc, 19, 2755-2761, 2015.

Dagan, G.: Linearized solutions of free surface groundwater flow with uniform recharge, J Geophys. Res., 72, 1183-1193, 1967.

Hansen, B. P., and Lapham, W. W.: Geohydrology and simulated ground-water flow, Plymouth-Carver Aquifer, southeastern Massachusetts, US Geological Survey, USA, Report 90-4204, 1992.

Hantush, M. S.: Growth of a ground water ridge in response to deep percolation, Symposium on Transient Ground water Hydraulics, Ft. Collins, Colorado, 25-27 July, 1963.

Hantush, M. S.: Growth and decay of groundwater-mounds in response to uniform percolation, Water Resour Res, 3, 227-234, 10.1029/WR003i001p00227, 1967.

Hsieh, P. C., Hsu, H. T., Liao, C. B., and Chiueh, P. T.: Groundwater response to tidal fluctuation and rainfall in a coastal aquifer, J Hydrol, 521, 132-140, 2015.

Illas, T. S., Thomas, Z. S., and Andreas, P. C.: Water table fluctuation in aquifers overlying a semi-impervious layer due to transient recharge from a circular basin, J Hydrol, 348, 215-223, 2008.

Ireson, A. M., and Butler, A. P.: A critical assessment of simple recharge models: application to the UK Chalk, Hydrol Earth Syst Sc, 17, 2083-2096, 2013.

Latinopoulos, P.: Analytical Solutions for Periodic Well Recharge in Rectangular Aquifers with 3rd-Kind Boundary-Conditions, J Hydrol, 77, 293-306, 1985.

Latinopoulos, P.: Analytical Solutions for Strip Basin Recharge to Aquifers with Cauchy Boundary-Conditions, J Hydrol, 83, 197-206, 1986.

Liang, X. Y., and Zhang, Y. K.: Analyses of uncertainties and scaling of groundwater level fluctuations, Hydrol Earth Syst Sc, 19, 2971-2979, 2015.

Liang, X. Y., Zhang, Y. K., and Schilling, K. E.: Analytical solutions for two-dimensional groundwater flow with subsurface drainage tiles, J Hydrol, 521, 556-564, 2015.

Manglik, A., Rai, S. N., and Singh, R. N.: Response of an Unconfined Aquifer Induced by Time Varying Recharge from a Rectangular Basin, Water Resour Manag, 11, 185-196, 1997.

Manglik, A., and Rai, S. N.: Two-Dimensional Modelling of Water Table Fluctuations due to Time-Varying Recharge from Rectangular Basin, Water Resour Manag, 12, 467-475, 1998.

Marino, M. A.: Hele-Shaw model study of the growth and decay of groundwater ridges, Journal of Geophysical Research, 72, 1195-1205, 10.1029/JZ072i004p01195, 1967.

Neuman, S. P.: Effect of partial penetration on flow in unconfined aquifers considering delayed gravity response, Water Resour Res, 10, 303-312, 10.1029/WR010i002p00303, 1974.

Ostendorf, D. W., DeGroot, D. J., and Hinlein, E. S.: Unconfined aquifer response to infiltration basins and shallow pump tests, J Hydrol, 338, 132-144, 2007.

Rai, S. N., Ramana, D. V., and Singh, R. N.: On the Prediction of Ground-Water Mound Formation in Response to Transient Recharge from a Circular Basin, Water Resour Manag, 12, 271-284, 1998.

Rai, S. N., Manglik, A., and Singh, V. S.: Water table fluctuation owing to time-varying recharge, pumping and leakage, J Hydrol, 324, 350-358, 2006.

Ramana, D. V., Rai, S. N., and Singh, R. N.: Water table fluctuation due to transient recharge in a 2-D aquifer system with inclined base, Water Resour Manag, 9, 127-138, 10.1007/BF00872464, 1995.

Rao, N. H., and Sarma, P. B. S.: Growth of Groundwater Mound in Response to Recharge, Ground Water, 18, 587-595, 1980.

Rao, N. H., and Sarma, P. B. S.: Recharge to Aquifers with Mixed Boundaries, J Hydrol, 74, 43-51, 1984.

Schmitz, G., and Edenhofer, J.: Semi Analytical Solution for the Groundwater Mound Problem, Adv Water Resour, 11, 21-24, 1988.

Singh, R.: Prediction of mound geometry under recharge basins, Water Resour Res, 12, 775-780, 10.1029/WR012i004p00775, 1976.

Singh, S. K.: Rate and volume of stream flow depletion due to unsteady pumping, J Irrig Drain E-Asce, 131, 539-545, 2005.

Tartakovsky, G. D., and Neuman, S. P.: Three-dimensional saturated-unsaturated flow with axial symmetry to a partially penetrating well in a compressible unconfined aquifer, Water Resour Res, 43, 2007.

van der Spek, J. E., Bogaard, T. A., and Bakker, M.: Characterization of groundwater dynamics in landslides in varved clays, Hydrol Earth Syst Sc, 17, 2171-2183, 2013.

Wang, C. T., and Yeh, H. D.: Obtaining the steady-state drawdown solutions of constant-head and constant-flux tests, Hydrol Process, 22, 3456-3461, 2008.

Yeh, H. D., Chang, Y. C., and Zlotnik, V. A.: Stream depletion rate and volume from groundwater pumping in wedge-shape aquifers, J Hydrol, 349, 501-511, 2008.

Yeh, H. D., and Chang, Y. C.: Recent advances in modeling of well hydraulics, Adv Water Resour, 51, 27-51, 2013.

Zlotnik, V., and Ledder, G.: Groundwater-Flow in a Compressible Unconfined Aquifer with Uniform Circular Recharge, Water Resour Res, 28, 1619-1630, 1992.

Zlotnik, V., and Ledder, G.: Groundwater Velocity in an Unconfined Aquifer with Rectangular Areal Recharge, Water Resour Res, 29, 2827-2834, 1993.

**Table 1.** Classification of existing analytical solutions involving localized recharge.

| References | Aquifer domain | Aquifer boundary conditions | Recharge | | Remarks |
|---|---|---|---|---|---|
| | | | Region | Rate | |
| | | *1D groundwater flow* | | | |
| Hantush (1963) | Infinite extent | None | Strip | Constant | |
| Rao and Sarma (1980) | Finite extent | Dirichlet | Strip | Constant | |
| Rao and Sarma (1984) | Finite extent | Dirichlet and no-flow | Strip | Constant | |
| Latinopoulos (1986) | Finite extent | Robin and Dirichlet/no-flow | Strip | Seasonal pulse | |
| Bansal and Das (2010) | Semi-infinite extent | Dirichlet | Strip | Constant | Sloping aquifer bottom |
| | | *2D groundwater flow* | | | |
| Hantush (1967) | Infinite extent | None | Rectangle | Constant | |
| Manglik et al. (1997) | Rectangle | No-flow | Rectangle | Arbitrary function of time | |
| Manglik and Rai (1998) | Rectangle | Dirichlet | Rectangle | Arbitrary function of time | |
| Bruggeman (1999) | Vertical strip | Robin | Strip | Constant | Laplace equation |
| Chang and Yeh (2007) | Rectangle | Dirichlet | Rectangle | Exponential decay | Sloping aquifer bottom |
| Bansal and Teloglou (2013) | Rectangle | Dirichlet at two adjacent sides and no-flow at the others | Rectangle | Exponential decay | Multiple recharges and pumping wells |
| | | *3D groundwater flow* | | | |
| Dagan (1967) | Infinite extent | None | Rectangle | Constant | Laplace equation; approximate solution |
| Zlotnik and Ledder (1993) | Infinite extent | None | Rectangle | Constant | Laplace equation |
| | | *Radial groundwater flow* | | | |
| Zlotnik and Ledder (1992) | Infinite extent with finite thickness | None | Circle | Constant | First-order free surface equation |
| Rai et al. (1998) | Circle | Dirichlet | Circle | Exponential decay | |
| Ostendorf et al. (2007) | Infinite extent with finite thickness | None | Circle | Exponential decay | First-order free surface equation |
| Illas et al. (2008) | Circle | Dirichlet | Circle | Exponential decay | Leaky aquifer |

**Table 2.** Default values of variables and hydraulic parameters used in the text.

| Notation | Default value (unit) | Definition |
|---|---|---|
| $h$ | None | Hydraulic head |
| $(x, y, z)$ | None | Variables of Cartesian coordinate |
| $t$ | None | Time |
| $(K_x, K_y, K_z)$ | (10 m/d, 10 m/d, 1 m/d) | Aquifer hydraulic conductivities in $x$, $y$, and $z$ directions, respectively |
| $(S_s, S_y)$ | ($10^{-5}$ $\mathrm{m}^{-1}$, 0.1) | Specific storage and specific yield, respectively |
| $I$ | 0.1 m/d | Constant recharge rate |
| $I_t$ | None | Transient recharge rate defined as $I_t(t) = I_1 + I_0 \exp(-rt)$ |
| $(I_1 + I_0, I_1)$ | (0.1 m/d, 0.05 m/d) | Initial and ultimate transient recharge rates, respectively |
| $r$ | $10^3$ $\mathrm{d}^{-1}$ | Decay constant of transient recharge rate |
| $(B, l, w)$ | (20 m, 1 km, 1 km) | Aquifer initial thickness and widths in $x$ and $y$ directions, respectively |
| $d$ | 50 m | Shortest distance between the edge of recharge region and an observation point |
| $(x_1, y_1)$ | 450 m | Location of bottom left corner of recharge region |
| $(a, b)$ | 100 m | Widths of recharge region in $x$ and $y$ directions, respectively |
| $(K_1, K_2, K_3, K_4)$ | 0.1 m/d | Hydraulic conductivities of media between aquifer and lateral boundaries 1, 2, 3 and 4, respectively |
| $(b_1, b_2, b_3, b_4)$ | 1 m | Widths of media between aquifer and lateral boundaries 1, 2, 3 and 4, respectively |
| $(d_1, d_2, d_3, d_4)$ | 450 m | Shortest distances from the edge of the region to lateral boundaries 1, 2, 3 and 4, respectively |
| $R$ | None | $\min(d_1, d_2, d_3, d_4)$ |
| $\bar{h}$ | None | $h/B$ |
| $\bar{R}$ | None | $R/d$ |
| $(\bar{x}, \bar{y}, \bar{z})$ | (12, 10, −0.5) | $(x/d, y/d, z/B)$ |

| | | |
|---|---|---|
| $\bar{t}$ | None | $K_x t/(S_s d^2)$ |
| $(\kappa_y,\ \kappa_z,\ \varepsilon)$ | (1, 0.625, 500) | $(K_y/K_x,\ K_z d^2/(K_x B^2),\ S_y/(S_s B))$ |
| $\xi$ | 0.1 | $I/K_z$ |
| $\xi_t$ | None | $\xi_1 + \xi_0 \exp(-\gamma \bar{t})$ |
| $(\xi_1,\ \xi_0,\ \gamma)$ | (0.05, 0.05, 2.5) | $(I_1/K_z, I_0/K_z,\ r S_s d^2/K_x)$ |
| $(\bar{l},\ \bar{w},\ \bar{a},\ \bar{b})$ | (20, 20, 2, 2) | $(l/d, w/d, a/d, b/d)$ |
| $(\bar{x}_1,\ \bar{y}_1)$ | 9 | $(x_1/d, y_1/d)$ |
| $(\kappa_1,\ \kappa_2,\ \kappa_3,\ \kappa_4)$ | 0.5 | $(K_1 d/(K_x b_1),\ K_2 d/(K_x b_2),\ K_3 d/(K_y b_3),\ K_4 d/(K_y b_4))$ |
| $(\bar{d}_1,\ \bar{d}_2,\ \bar{d}_3,\ \bar{d}_4)$ | 9 | $(d_1/d, d_2/d, d_3/d, d_4/d)$ |

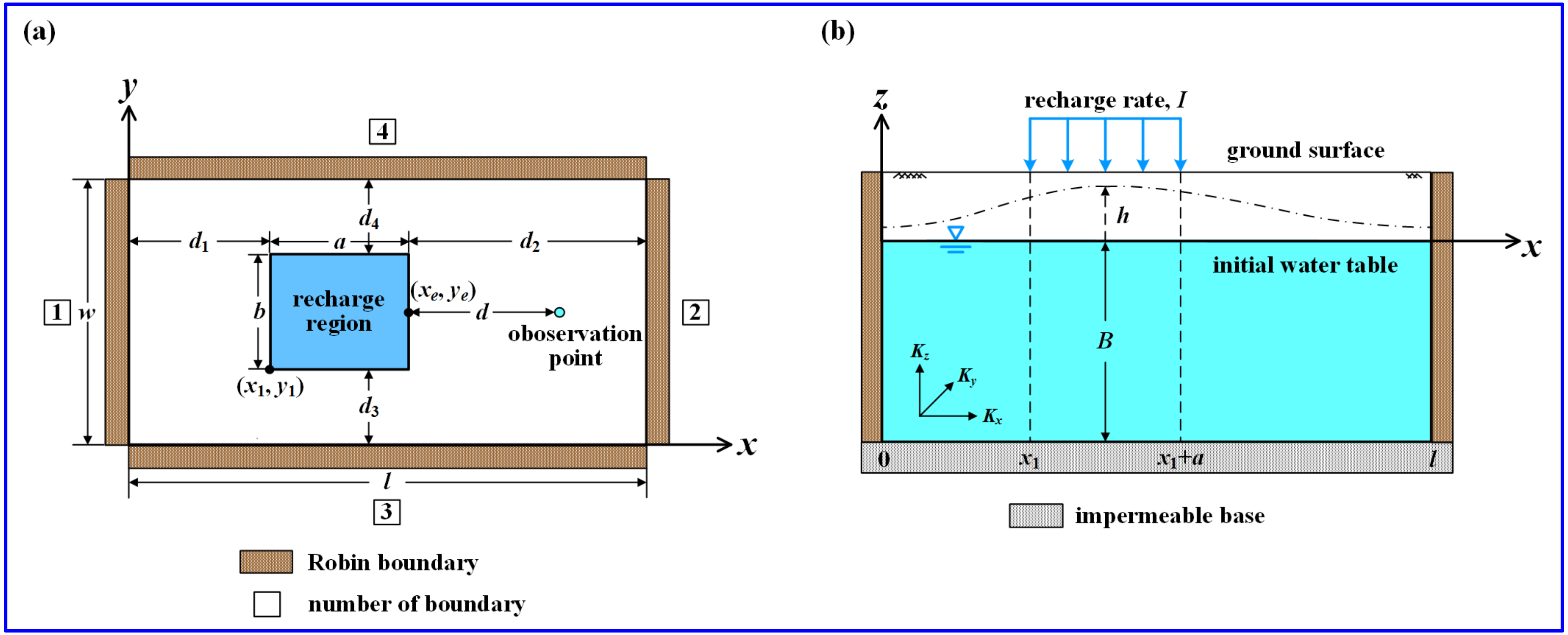


**Figure 1.** Schematic diagram of a rectangular-shaped unconfined aquifer with localized recharge (a) top view (b) cross section view.

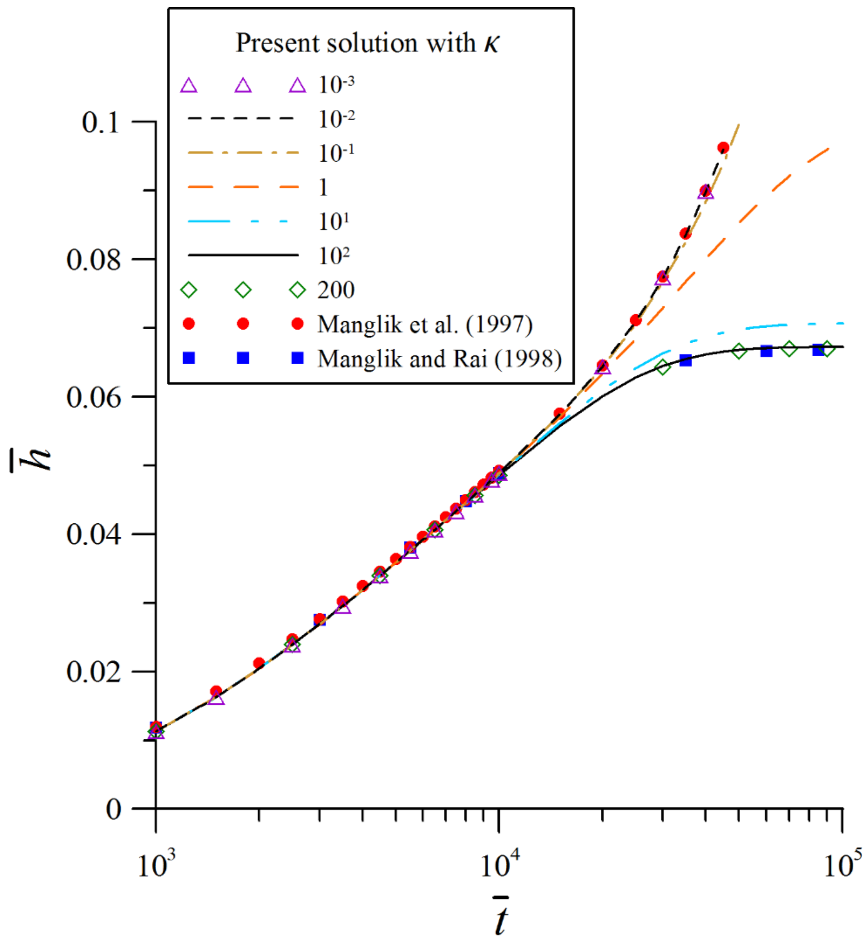


**Figure 2.** Temporal distributions of the dimensionless head predicted by Manglik et al. (1997) solution for a no-flow boundary, Manglik and Rai (1998) solution for a Dirichlet boundary, and the present solution with $\kappa_z = 1$ for a Robin boundary.

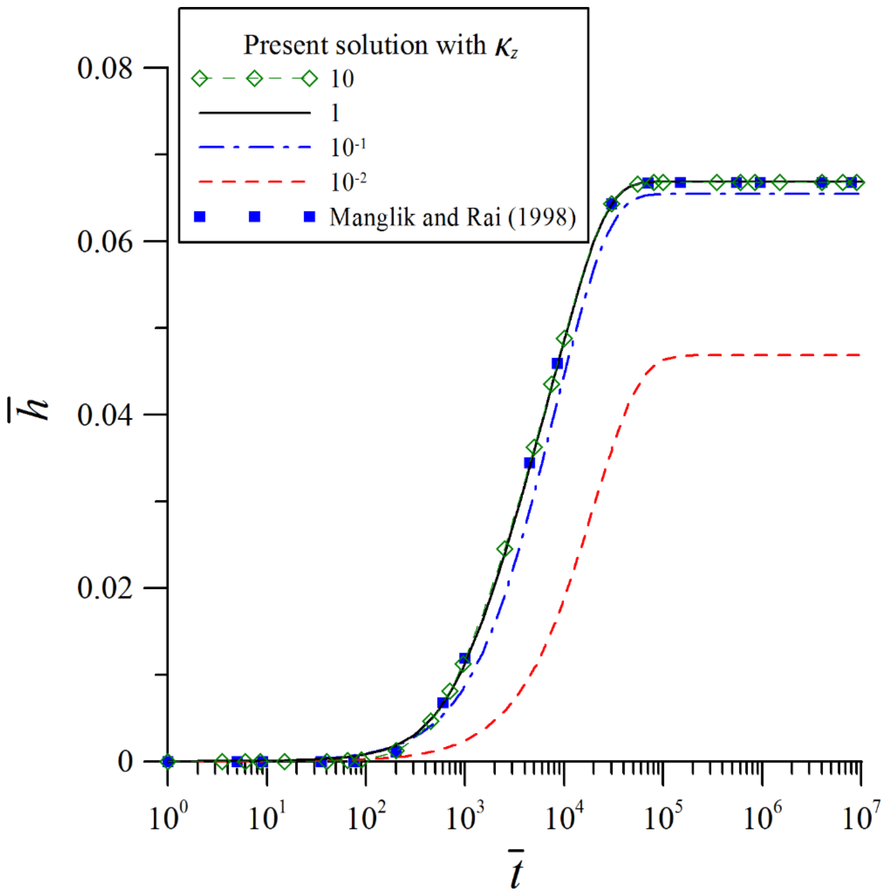


**Figure 3.** Temporal distributions of the dimensionless head predicted by Manglik and Rai (1998) solution based on 2D flow and the present solution for 3D flow with various $\kappa_z$.

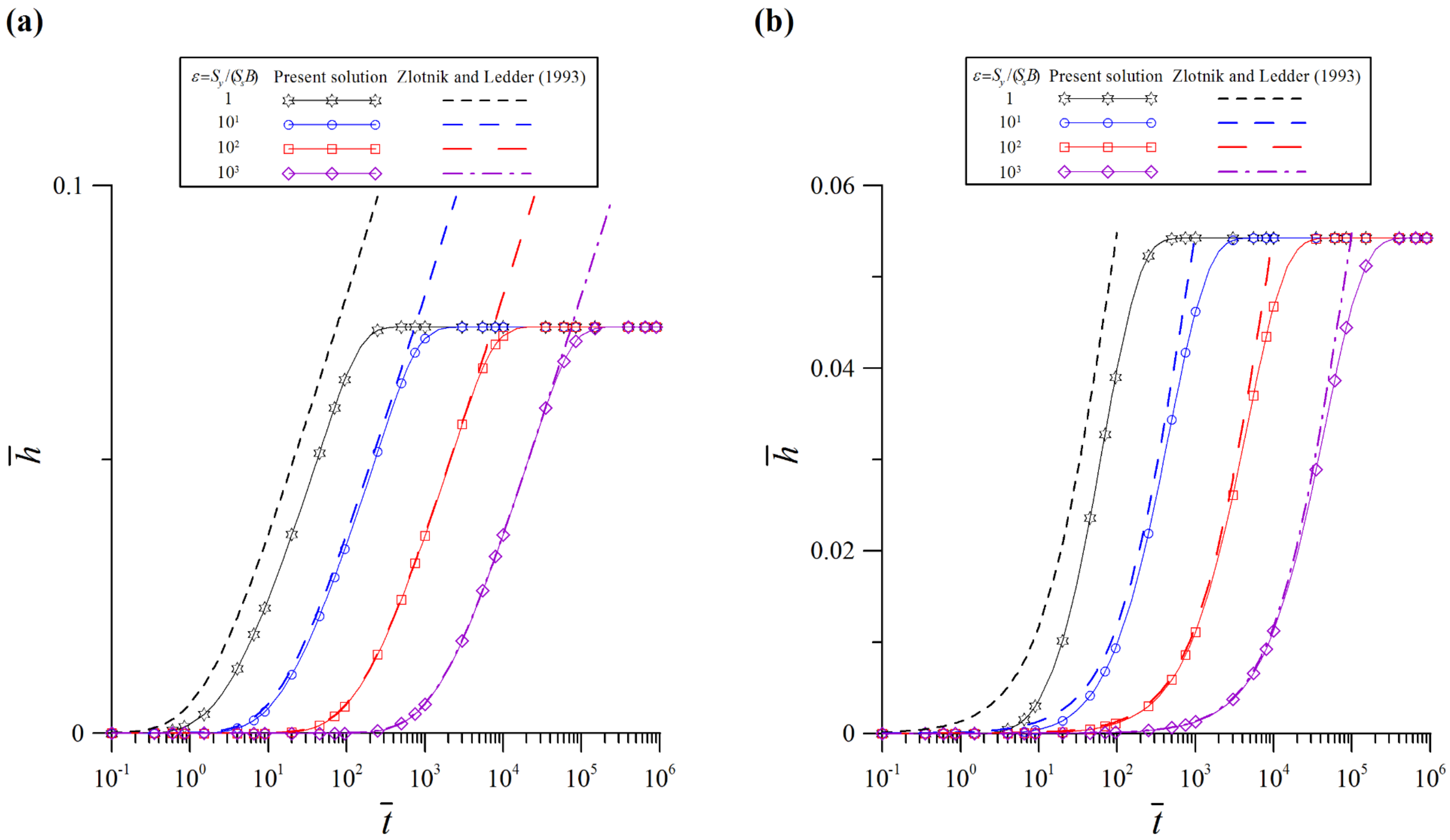


**Figure 4.** Temporal distributions of the dimensionless head for (a) $\kappa_z = 10^{-2}$ and (b) $\kappa_z = 10$ predicted by Zlotnik and Ledder (1993) solution based on the assumption of $S_s = 0$ and the present solution relaxing the assumption.

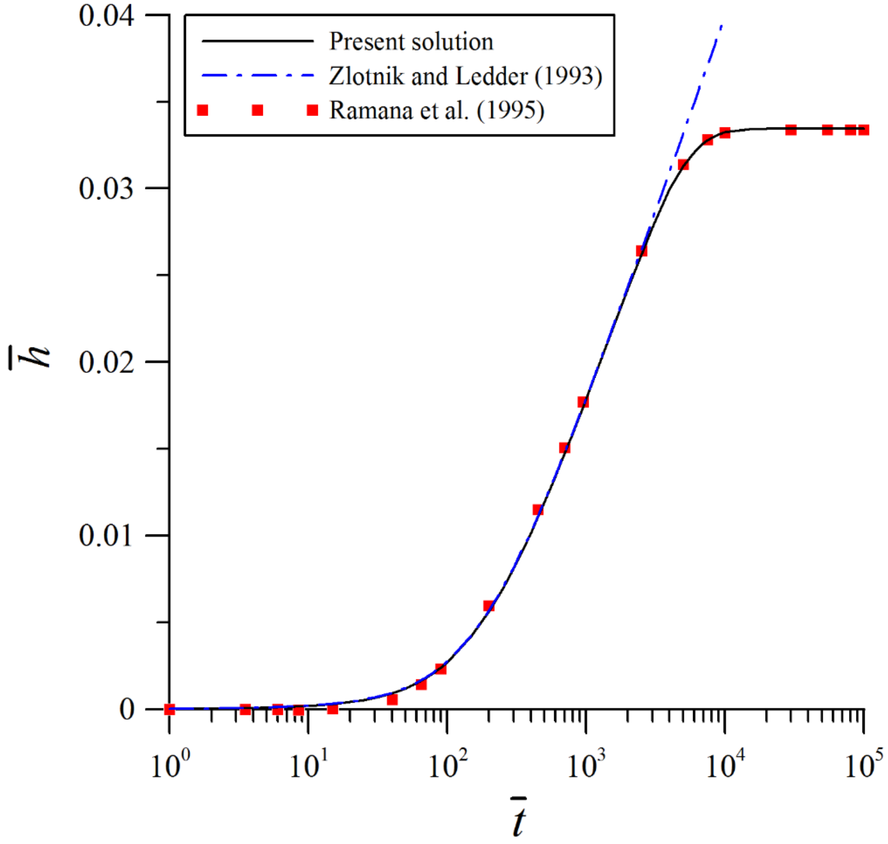


**Figure 5.** Temporal distributions of the dimensionless head subject to a transient recharge rate predicted by Ramana et al. (1995) solution, Zlotnik and Ledder (1993) solution, and the present solution with $\kappa_z = 1$, $\kappa = 100$, and $\varepsilon = 100$.

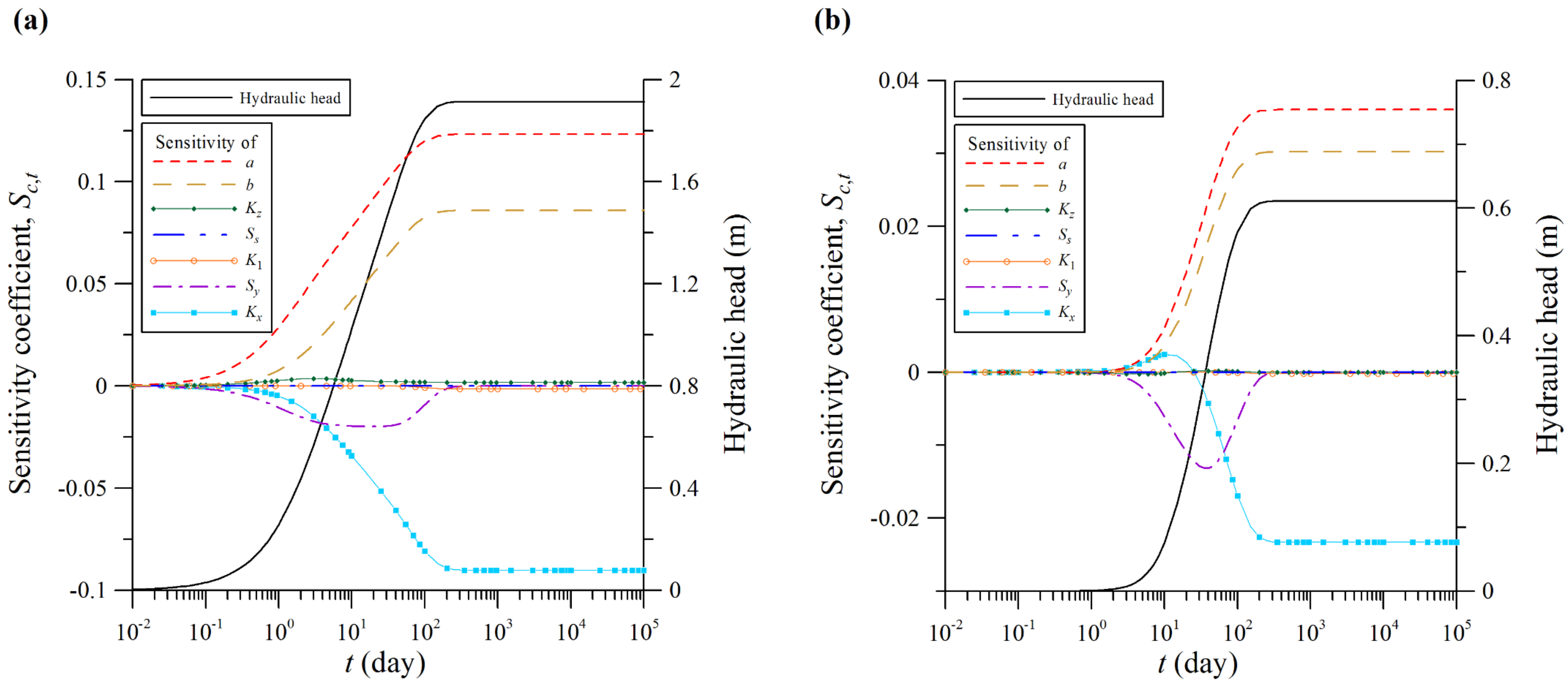


**Figure 6.** Temporal distributions of the normalized sensitivity coefficients of the hydraulic head at the observation points of (a) ($x$, $y$, $z$) = (555, 500, −10) and (b) ($x$, $y$, $z$) = (800, 500, −10) to the changes in parameters $a$, $b$, $K_z$, $S_s$, $K_1$, $S_y$, and $K_x$.